Icelandic
Meteorological Office

Veðurstofa
Íslands

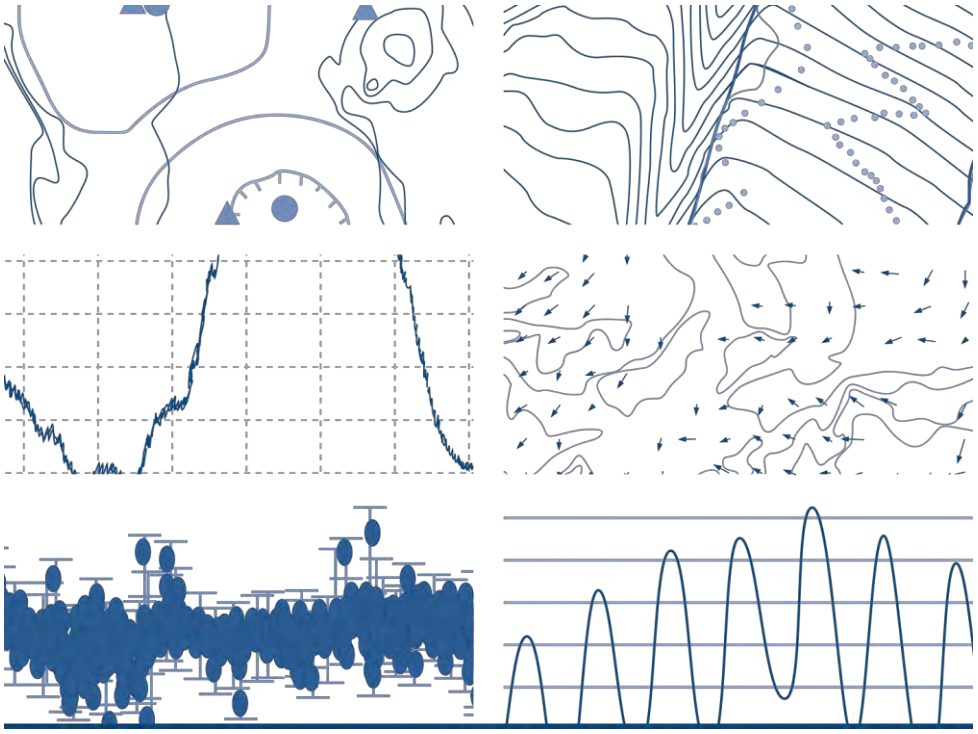

Development and Implementation of Seismic Early Warning Processes in South-West Iceland

Kristín S. Vogfjörd
Einar Kjartansson
Ragnar Slunga
Páll Halldórsson
Sigurlaug Hjaltadóttir
Gunnar B. Gudmundsson
Hjörleifur Sveinbjörnsson
Sigþrúður Ármannsdóttir
Bergþóra Thorbjarnardóttir
Steinunn S. Jakobsdóttir

Report

VÍ 2010-012

Icelandic
Meteorological Office

Veðurstofa Íslands

Development and Implementation of Seismic Early Warning Processes in South-West Iceland

Kristín S. Vogfjörd, Icelandic Met Office
Einar Kjartansson, Icelandic Met Office
Ragnar Slunga, QuakeLook AB Stockholm
Páll Halldórsson, Icelandic Met Office
Sigurlaug Hjaltadóttir, Icelandic Met Office
Gunnar B. Gudmundsson, Icelandic Met Office
Hjörleifur Sveinbjörnsson, Icelandic Met Office
Sigþrúdur Ármannsdóttir, Icelandic Met Office
Bergþóra Thorbjarnardóttir, Icelandic Met Office
Steinunn S. Jakobsdóttir, Icelandic Met Office

Report

Veðurstofa Íslands
Bústaðavegur 9
150 Reykjavík

+354 522 60 00
+354 522 60 06
vedur@vedur.is

VÍ 2010-012
ISSN 1670-8261

Veðurstofa Íslands

Keypage

Report no.:	**Date.:**	**ISSN:**	**Public** ☒ **Restricted** ☐
VÍ 2010-012	December 2010	1670-8261	**Provision:**

Report title / including subtitle	**Number of copies:**
Development and Implementation of Seismic Early Warning Processes in SW-Iceland – SAFER	25
	Pages: 83
Authors: Kristín S. Vogfjörd, Einar Kjartansson, Ragnar Slunga, Páll Halldórsson, Sigurlaug Hjaltadóttir, Gunnar B. Gudmundsson, Hjörleifur Sveinbjörnsson, Sigthrúdur Ármannsdóttir, Bergthóra Thorbjarnardóttir, Steinunn S. Jakobsdóttir	**Managing director** Jórunn Harðardóttir
	Project manager: Kristín S. Vogfjörð
Project phase: Research, modelling of seismological data	**Project number:** 2811-0-0005

Report contracted for:

European Commission, under 6th Framework Project-'SAFER', Contract No. 036935.

Summary:

Early warning, real time or near-real time (RT, NRT) automatic analysis processes have been developed for determination of earthquake location and magnitude as well as mapping of shaking, intensity and stress in Iceland. These processes include: **(i)** Automatic NRT relative relocation, developed and installed in the Hengill test region; **(ii)** RT determination of dominant period in P-waves for estimation of earthquake magnitude; **(iii)** determination of the relationship between seismic intensity and peak ground acceleration and peak ground velocity (*PGA* and *PGV*); **(iv)** RT web publishing of *Alert Map*, based on PGV and PGA attenuation relations, RT determination of *PGV*, *PGA* and *P*-wave arrival times at seismic stations and central processing to determine earthquake location and magnitude within minutes of an earthquake; **(v)** immediate, automatic web publishing of ground shaking and intensity based on the output parameters of *Alert Map*, maps of V_s^{30} velocities in Iceland and the USGS' s *ShakeMap* software; **(vi)** development and testing of stress mapping on N-S faults in southwest Iceland.

Keywords:

Iceland, earthquakes, seismic early warning, automatic, real time, near real time, relative earthquake location, fault mapping, magnitude, dominant frequency, intensity, peak ground velocity, peak ground acceleration, Alert map, ShakeMap, stress mapping

Managing director's signature: Jórunn Harðardóttir

Project manager's signature: Kristín S. Vogfjörð

Reviewed by:

Contents

SAFER Rannsóknaverkefnið

Í Evrópusamstarfsverkefninu SAFER (*Seismic eArly warning For EuRope*) var unnið að rannsóknum og þróun á rauntímaúrvinnslu jarðskjálftabylgna um leið og þær berast í mælistöðvar í því markmiði að þróa ferla sem geta nýst til viðvarana og viðbragða áður en stærstu og skæðustu jarðskjálftabylgjurnar berast til viðkvæmra mannvirkja eða þéttbýliskjarna, þar sem þær geta skapað hættu. Þátttakendur voru frá helstu jarðskjálftarannsóknastofnunum Evrópu og þeim löndum álfunnar þar sem jarðskjálftavá er mest. Veðurstofa Íslands var þátttakandi í verkefninu og vann að þróun rauntímaferla fyrir bráðaskjálftaviðvörun (*e. seismic early warning*) á suðvesturlandi. Helstu niðurstöður rannsóknanna voru settar fram í nokkrum smáskýrslum (*e. deliverables*), sem var skilað sem afurðum Veðurstofunnar í verkefninu. Þessum smáskýrslum er safnað saman í tvær skýrslur, þar sem sú fyrri inniheldur niðurstöður um dvínun hraða og hröðunar með fjarlægð frá upptökum jarðskjálfta, en sú síðari er um: 1) þróun sjálfvirkrar kortlagningar sprungna í nær-rauntíma, 2) rauntímamat á stærð jarðskjálfta byggt á ráðandi tíðni í P-bylgjum (*ElarmS*), 3) samband milli skjálftaáhrifa og mesta hraða og hröðunar, 4) þróun sjálfvirkra, rauntíma „alert“ korta og hristingskorta (*ShakeMap*) fyrir jarðskjálfta, 5) undirbúning rauntímakortlagningar á eftirskjálftavá, og 6) rauntímakortlagningu spennuútlausnaskjálfta. Upplýsingar um SAFER verkefnið má finna á vefsíðunni: http:// www.saferproject.net/.

1. Development and implementation of near-real time automatic fault mapping in SW-Iceland

Project no. **036935**

Project acronym: **SAFER**

Project title: **Seismic eArly warning For EuRope**

Instrument: **Specific Targeted Research Project**

Thematic Priority: **Sustainable development, global change and ecosystem priority 6.3.iv.2.1: Reduction of seismic risks**

D2.27 Results of the application of the automatic fault mapping procedure to a few large earthquakes in SW-Iceland

Kristín S. Vogfjörd,[1)] Sigurlaug Hjaltadóttir,[1)] Ragnar Slunga[2)] and Gunnar B. Gudmundsson[1)]
[1)] Icelandic Meteorological Office
[2)]QuakeLook AB Stockholm

Results of the application of the automatic fault mapping procedure to a few large earthquakes in SW-Iceland

Introduction

During the 18 year operation of the SIL automatic seismic system in Iceland, the network has recorded foreshocks before all medium to large earthquakes in SW-Iceland. If such foreshocks can be located with high-precision before the following main shock occurs, the foreshocks may already have delineated the fault plane of the coming main shock, thus allowing its fault plane to be immediately inferred and providing early-warning mechanism information.

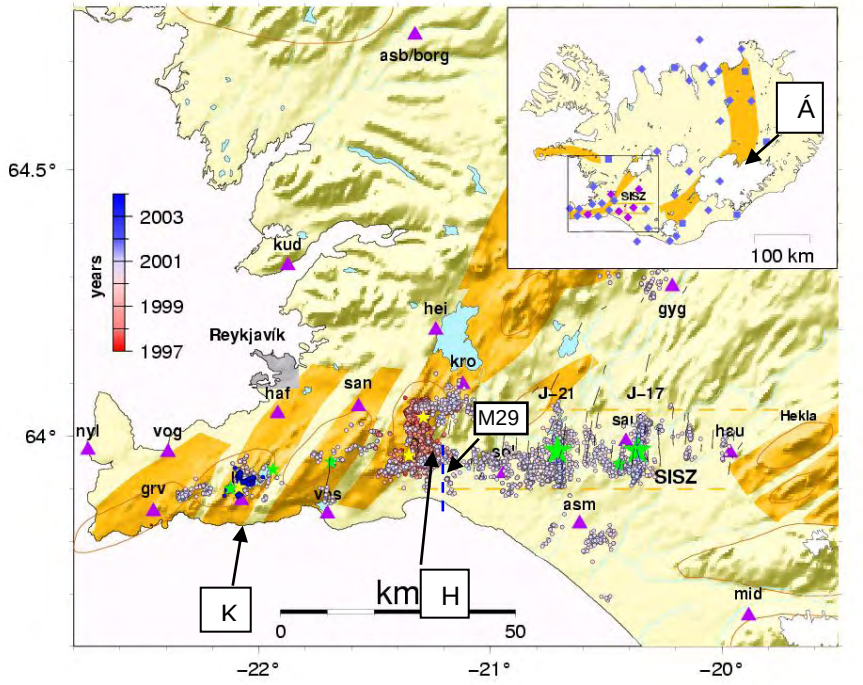

Figure 1. Map showing SW-Iceland, the focus area within SAFER. Seismicity during 1997–2000, defining many of the already mapped faults, is shown colour coded according to age. Events with M>5 are shown as stars. The outline of the South Iceland Seismic Zone (SISZ) is shown with orange dashed lines. Test sites are marked on the map with letters K, H, Á, J-17, J-21 and M-29. Locations of seismic stations are also sown (purple triangles).

High-precision earthquake locations, with optimum achievable location accuracy on the order of tens of meters are currently obtained through relative relocation (double difference) of manually located earthquakes (Slunga et al., 1995; Hjaltadóttir and Vogfjörd, 2005). The objective is to obtain this location accuracy in near-real time in the SAFER region of SW-Iceland (see Figure 1) by starting with the less accurate automatic event locations, available 2

minutes after the origin time (OT), and further developing the existing relative location method to operate automatically and in near-real time. The procedure will make use of the existing database of waveforms from previous relatively located events, many of which have already been used to map sub-surface faults. Using this approach earthquakes can be automatically located with high precision, they can possibly be associated with previously mapped faults, or can illuminate new faults, all in near-real-time.

Procedure

Around 100 major and minor sub-surface faults have already been mapped in SW-Iceland through relative relocation of over 50 thousand manually located microearthquakes. A selection of representative events from this database is used to construct a library, against which all new events will be compared. The selection is made on the basis of small relative location error of events on already mapped faults and small absolute error of other events.

Due to the requirement of near-real time results, the procedure will use automatic earthquake locations. The automatic locations are based on phase information, which is transmitted in real-time from the seismic stations to the data center in Reykjavík, and they are available at ~OT+2 minutes. Waveforms arrive within another 5-to-15 minutes. When waveforms from two or more stations have arrived, each new event is compared to a subset of near-by events from the event library via cross-correlation of P and S waveforms. The relative times are inverted for best location, resulting in a high-precision automatic location for the new event available within minutes. As more waveforms arrive, the process is repeated to improve the location. The location accuracy that can be achieved is from tens of meters to a few hundred meters, thus enabling the delineation of active faults in near-real time. Foreshocks preceding a large earthquake by more than 20 minutes will already have been located with high precision before the main shock occurs, and may already have delineated the fault plane of the coming main shock, thus allowing its faulting mechanism to be immediately inferred. Due to its size, the main shock will not correlate with events from the library, but the aftershocks will, and as they start to accumulate their subsequent high-precision location will quickly confirm the fault plane.

The relative location code has been adapted to invert for best location of one new automatically located event relative to a subset of near-by library events. Waveforms from the new event are cross-correlated with the waveform library, and arrival times of P and S waves from the new event relative to the 40 highest correlating library events are subsequently inverted for the best location. In its present testing form the procedure takes about 4 minutes to complete, comparing a few hundred library events to 4 new waveforms (stations) and 8 minutes to 8 new waveforms. The code is still in the developmental stage and not optimized for short run-time. When fully optimized the processing time is expected to at least halve the present run-time. Furthermore, as IMO moves to continuous transmission of all waveform data in the coming years, the waiting time for waveforms to arrive (~15 minutes) will be greatly reduced.

Testing of the procedure

The procedure is being tested for robustness in improving event location and for ability to delineate faults of coming main shocks using the foreshocks that have been recorded before the major events. To test the robustness, tests sites were selected in three different areas; two sites

in SW-Iceland where extensive fault mapping has been performed, on the Reykjanes peninsula and in the Hengill region (marked with letters K and H on the map in Figure 1). The third site, Álftadalsdyngja in the Northern Volcanic Zone (NVZ) (marked with Á in Figure 1), has produced intense earthquake swarms due to magma movements at mid-crustal levels during the last year. Test sites for automatic fault-mapping with foreshocks of large events, were selected from three locations in the SISZ; the M_L6.5 event on June 17 and the M_L6.4 event on June 21, 2000 and the recent M_L6.3 event on May 29 in 2008 (marked with J-17, J-21 and M-29 on Figure 1). In general the results show that the procedure is robust and that for some major events, the foreshocks do delineate the fault plane.[1]

Robustness

Results from the Kleifarvatn test site (K) are shown on the map in Figure 2. Original relatively located events following an M_L5.0 event in August 2003 on a 6 km long NS striking, vertical, strike-slip fault are shown in orange. From this dataset 320 library events (black circles) with absolute location accuracy < 100 m are selected. Three recent M1.6 events, with original, automatic location shown with white symbols, are relatively relocated with respect to the library events, using cross-correlation of waveforms from 4 (light blue) and 8 (dark blue) closest stations, respectively. The 40 highest correlating events are then inverted for the best location. For comparison the manual locations, obtained by an analyst are shown in yellow. The final locations of the events are all within an approximately 1 km^2 area, even though their original, automatic locations are up to 5 km away. They are also within a few hundred meters from the manual locations, which have a location accuracy of 200-400 m. The locations improve, by a few hundred meters, by going from 4 to 8 stations, but even with the four stations, the location accuracy is at least as good as the manual location. The relocation takes 4 minutes using 4 stations and twice as long using 8 stations.

Results from the Hengill area test site (H) are displayed on the map in Figure 3. 160 library events (black circles) from an earthquake swarm in 1997 were selected; 40 from each of four already mapped sub-surface faults shown (orange and green). Four, more recent events of varying magnitudes ($0.5 \leq M \leq 2.5$) were relocated with respect to the library set. Their original automatic locations are shown with white stars, scaled by magnitude. The relative relocation is shown in blue and the manual location in yellow. All events move by a few hundred meters up to a kilometer to an improved location, and to within 500 m of the manual location (yellow). Two of the four events (from 1998) fall on the pre-mapped faults. These events had also previously been relatively relocated from their manual location. For comparison these locations are shown in gray. They are within 200 m from the test results. Even the locations of two events outside the library data set, which do not belong to any of the four faults, improve by several hundred meters.

[1] All M_L estimates are based on the attenuation relationship of PGV with distance developed in SAFER deliverable D5.2 (Pétursson et al., 2008).

The tests performed on two M~0 events in the Álftadalsdyngja region in the NVZ showed similar location improvements as the other two test areas. The region has been experiencing a magmatic intrusion resulting in strong earthquake swarm activity at 1318 km depth during the last year. Waveforms from four stations representing two shallow (h<5 km), M~0 events, were compared to waveforms from 200 library events at 11–17 km depth. The original automatic locations were 4 and 6 kilometres away from the library set. One event relocated into the library data set, at 15 km depth and within a kilometre of the manual location; the other moved 1 km towards the library set, remained shallow and relocated to within 2 km of the manual location (see Vogfjörd et al., 2008).

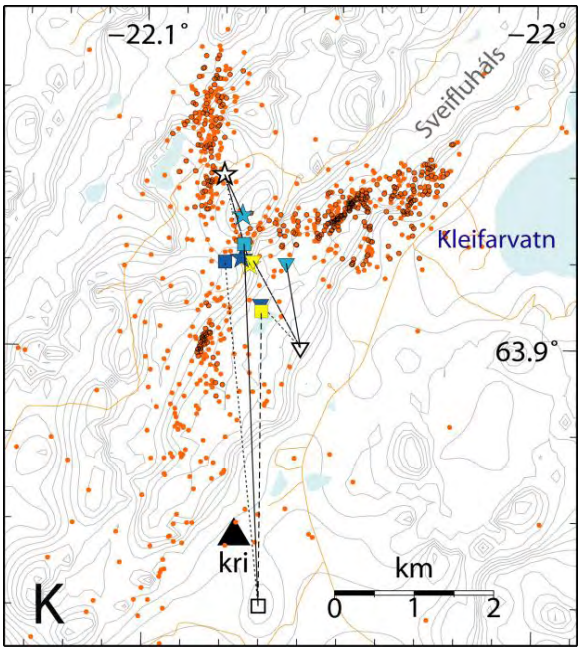

Figure 2. Test site K-Kleifarvatn area showing relocation of three events. White symbols denote the original, automatic location, yellow symbols the manual location and blue relative locations, using wave forms from 4 (light blue) and 8 (dark blue) stations, respectively.

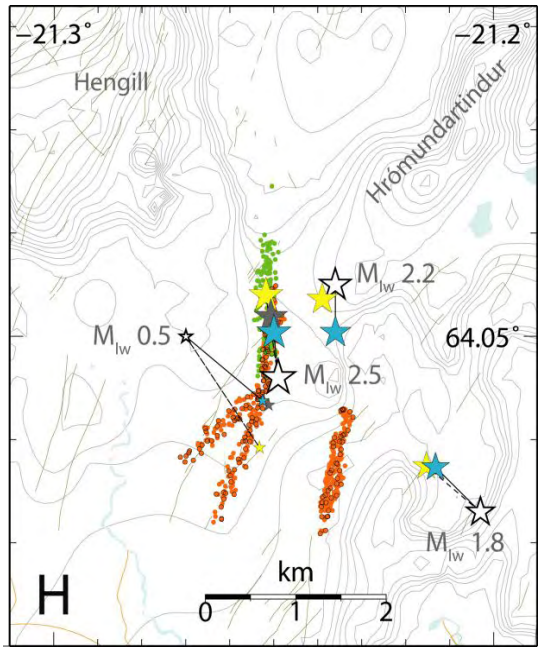

Figure 3. Test site H-Hengill area showing relocation of four events. Same colour scheme as in Figure 2. The relocated events are scaled with size.

Fault mapping

Examination of the capability of a high-precision foreshock distribution, preceding a large earthquake, to constrain the fault plane of the on-coming main shock was done by relatively relocating foreshock sequences of three large earthquakes (M_L6.3 and 6.5) in the SISZ. Their locations are shown on Figure 1. Two (J-17 and J-21) are from June 2000 and one (M29) is from May 2008.

The results from the 17 June 2000, Holt fault (J-17), which ruptured in an M_L6.5 event along a 12-km-long, N7˚E, vertical strike-slip fault, are shown on the map in Figure 4. The large open star shows the epicenter of the main event and a smaller star shows the epicenter of a second M_L5.7 event, which occurred 2 minutes later on a shorter, similarly striking fault, 3.5 km farther west. Based on previous relative locations of aftershocks from the year 2000, the J-17 fault was shown to be composed of three vertical, *en echelon* fault segments of approximately equal length, each with a more easterly strike than the whole fault (Hjaltadóttir and Vogfjörd, 2005). The hypocenter of the main event falls at the center of the middle segment. In the figure, gray circles show the location of the relatively relocated aftershocks during year 2000 and black circles represent the library subset. Orange, filled circles represent earthquakes between January and May 2000 and green circles denote events during 1–17 June.

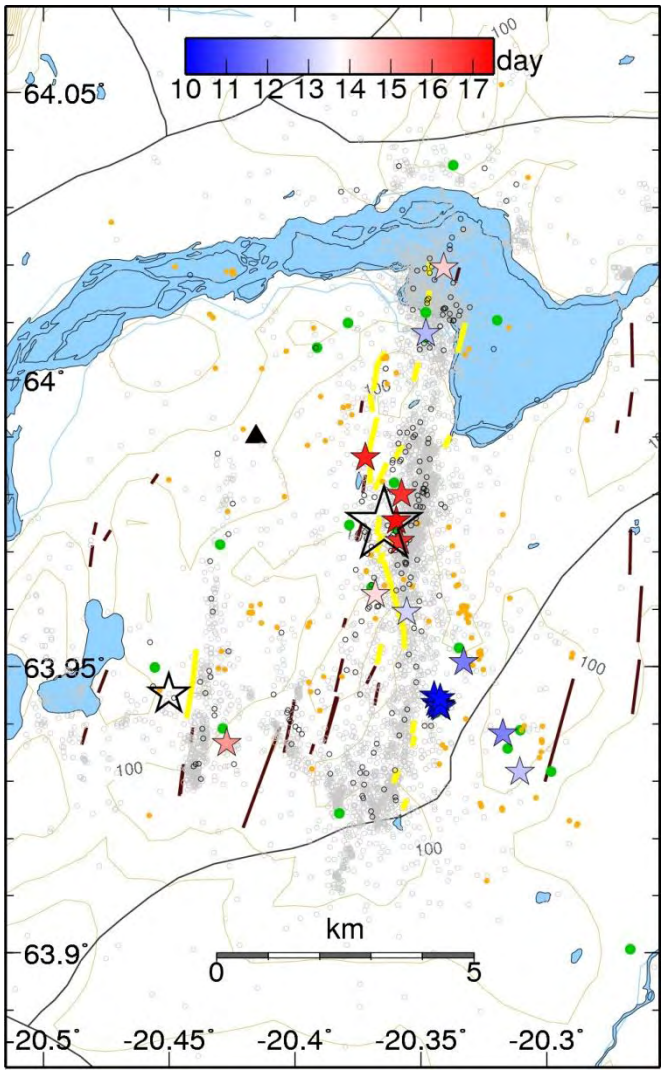

Figure 4. Test site J-17 showing the 17 June 2000, ML6.5 fault and the ML5.7 (2-minute) fault. Open gray circles denote relocated aftershocks from year 2000. Black open circles denote the library data set. Orange circles show events occurring January through May 2000, and larger green filled circles show earthquakes occurring during June 1-17, before the main shock. Its epicenter is marked by a large star; a smaller star marks the epicenter of the ML5.7 event occurring 2 minutes later. The coloured stars show the time and location of 20 test events, which occurred between 10 and 17 June. These events are coloured according to date, with the colour scale shown at the top. Mapped surface ruptures associated with the J-17 event are shown as yellow lines (Clifton and Einarsson, 2005).

Automatic locations of 20 earthquakes in the nearest vicinity of the fault, occurring before the main shock, during 10–17 June were relocated using all available waveforms. The results, displayed as stars, are colour coded according to date of occurrence. Upon relocation, most of the test events stay roughly within a kilometers distance from their original location, except for two events. Their locations improve dramatically as they respectively move 2 km towards the northern end, and 7 km towards the center of the fault.

During the five-and-a-half months preceding the J-17 earthquake, the seismicity was mostly distributed between the two Holt faults (J-17 and the 2-minute fault), as well as extending approximately from the center of the main fault towards SE along a N152°E direction. In the final week before the earthquake, the activity suddenly picked up in this region, as seven tightly clustered events occurred there on 10 June (dark blue stars). Three more events followed near this location during the next two days, and then moved towards the center of the fault during another two days. About the same time, two events occurred at the northern end of the fault, in addition to one event on the 2-minute fault. During the final 19 hours, on 16 and 17 June, three events (red stars) occurred around 7-km-depth very close to the main shock's hypocenter, and a fourth event 1 km deeper and farther northwest. The last one of these foreshocks occurred roughly 8 hours prior to the main event. Therefore, all four could have been relatively located before the main shock struck. The magnitudes of the last four events are around 0 except for the last one, which had a magnitude close to 1. Based only on the seismicity concentration in the preceding 19 hours, an approximate N-S fault strike could have been assumed for the following M_L6.5 event, but considering a longer period, the fault strike becomes harder to infer from the foreshock distribution.

Following the pattern of historical seismicity, aftershocks of the J-17 earthquake migrated westwards, with seismicity concentrating in two main areas, one of which was the epicentral area of the J-21 earthquake, which struck 3½ days later, on 21 June. IMO issued a warning 26 hours prior to the earthquake, based on the distribution of automatic and available manual event locations, stating that the next large earthquake was most likely to take place in the J-21 epicentral area, with a second, less likely location 5 km farther west (Stefánsson et al., 2000). Figure 5 shows relatively relocated events during the year 2000 on the J-21, Hestvatn fault as gray circles. The event distribution defines two overlapping fault segments with a common NS-directed strike, but differing dip; a southern vertical section and an eastward dipping northern section (Hjaltadóttir and Vogfjörd, 2005). Foreshocks occurring during the 24 hours preceding the J-21 event are colour coded according to age. Most of them were located along the E-W trending conjugate fault revealed by the mapped surface ruptures (Clifton and Einarsson, 2005), but of the 11 events occurring during the final two hours, 6 occurred near the bottom of the northern fault section and of those, 4 were in the same location just below the hypocenter of the main event. One shallow event appears to have been located on the dipping fault section. These events were mostly of magnitude around 0.5, but the last two, located at the epicenter, were around magnitude 1. The last foreshock occurred 13 minutes before the main event, so all the foreshocks could possibly have been relatively located before the main event stuck. Furthermore, considering only the final 2 hours preceding the earthquake (orange and red on the map in Figure 5), the event distribution appears to define the fault strike of the main event.

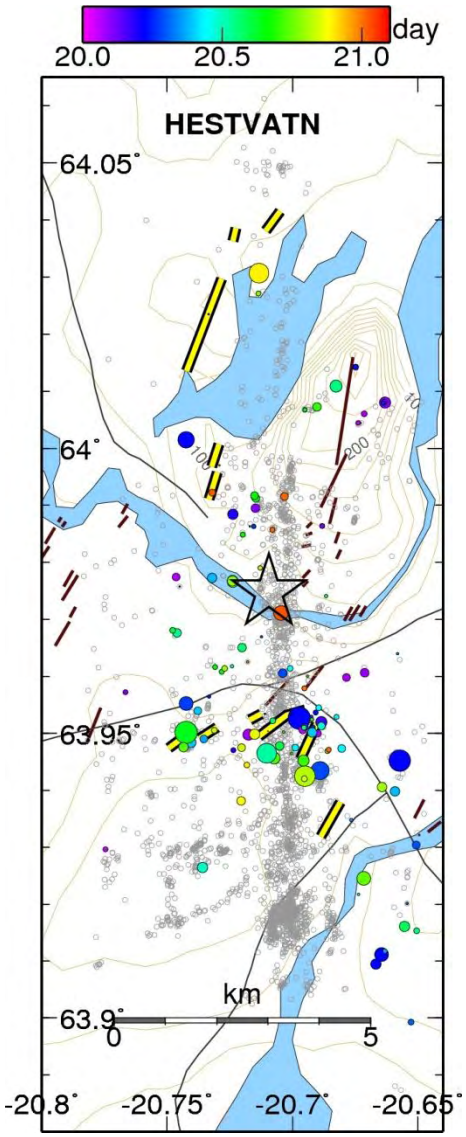

Figure 5. Relocated earthquakes on and near the 21 June Hestvatn fault (grey circles). The epicenter of the M_L6.4 earthquake, shown with an open star is at the center of the fault. Locations of the approximately 140 foreshocks which occurred during the 24 hours before the main event are colour coded according to time, with the time scale shown at the top. Most of the foreshocks are located along the E-W conjugate fault extending westwards from the main fault. Mapped surface ruptures are shown as yellow lines (Clifton and Einarsson, 2005).

The last major earthquake in Iceland occurred in the western part of the SISZ (marked as M29 on Figure 1) on 29 May 2008. It was actually two nearly simultaneous earthquakes, 4 km apart, with a combined magnitude of M_L6.3. Both faults were vertical, oriented N-S, and with right-lateral strike-slip motion. Around 1300 of the aftershocks recorded during the first six days, have been manually located. These events were relatively relocated together with the seismicity during the first half of the year. The results are shown on Figure 6, where the events have been colour coded according to time of occurrence during the year. The manual location of the epicenter of the main event is shown with a star. The aftershocks are shown as circles, while all earthquakes preceding the main shock are shown as squares. The foreshocks were not individually relocated with library events, as would have been the case had the automatic procedure been implemented. However, the relocation of their manual location shows that the strike and dip of the triggering fault could have been delineated before the event struck. The event started on the eastern (Ingólfsfjall) fault and the waves from this event triggered the motion on the western (Kross) fault, presumably at its center. It is possible that the E-W oriented fault west of the Kross fault (previously mapped by seismicity in 1998), which is delineated by the aftershocks was also active in the event, but so far aftershocks on this fault have not been found in the data until 53 minutes after the main event. The other two faults, however, start to generate aftershocks immediately after the event.

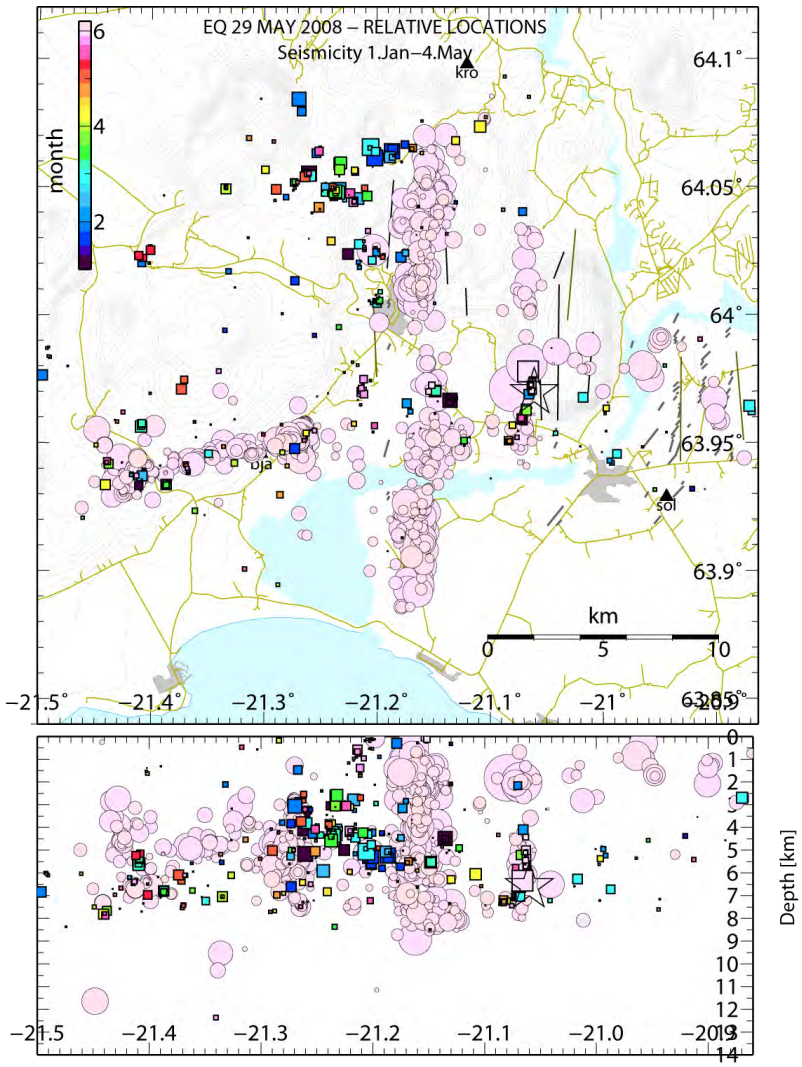

Figure 6. Map view (upper) and vertical view (lower) of relatively located earthquakes from 2008 in the region of the 29 May 2008 earthquake. Events are colour coded according to age, with the colour scale shown in the upper left corner. The main event and aftershocks are shown with circles, while events before the main event are shown as squares. A star shows the initial, manual location of the main event. Waveforms from the main event do not correlate with waveforms from the other smaller events and therefore its relocation near the surface is not well constrained.

During the five months preceding the earthquake there were on average 5 microearthquakes per month on or around the two N-S faults. The seismicity was distributed over the Kross fault, but concentrated towards the southern end of the Ingólfsfjall fault, where in late April a swarm of 12 events occurred. No activity was on either fault the day before the main earthquake, but 13 hours prior to its origin time (OT) there was an M0.3 event at the center of the Kross fault. Then around 8,5 hours before OT, two events (-0.1 <M<0.5) occurred in the epicentral area of each fault. After that no foreshocks are recorded on the Kross fault. On the Ingólfsfjall fault, however, an M0.3 event occurred 4 hours before OT and an M3.1

earthquake 1 hour before OT. This event was immediately followed by a swarm of activity, producing 40 events in all; two events of M~1.1, the remaining between -0.1 and 0.3.

The relative location of the last earthquake swarm shows a distribution of approximately 900m N-S and a vertical extent of 1 km at around 5.5 km depth. At OT-20 minutes, nearly 30 events had already occurred. With the automatic relocation process in operation, these events could already have been relatively located, before the main event struck, and the fault plane of the Ingólfsfjall fault could therefore have been immediately inferred. The fault plane of the triggered event (Kross fault), however, could not have been foreseen.

Conclusions

In general, the test results from all sites show that the automatic relative relocation procedure is robust. Using waveforms from only a few stations (4-8), events originally located up to several km away from their optimum locations are drawn to within a few hundred meters of the manual location, which generally has a location accuracy of a few hundred meters. When fully optimized, the run-time will decrease and then the procedure is expected to take only a few minutes. It will be implemented to run automatically in near-real time, providing location accuracy on the order of 100´s of m within minutes of an event. Therefore, if a large event has several foreshocks preceding it by 20 minutes or more, high-precision locations of the foreshocks can be obtained before the main event occurs.

The tests of the foreshock distributions' ability to constrain fault-planes of the following large events indicate that in some cases, when several foreshocks occur within the time window 20 minutes to approximately 24 hours before the main event, the procedure can enable rough mapping of the fault strike and sometimes also the dip, and thus provide an immediate estimate of the fault plane.

Mechanisms are calculated for all located earthquakes in Iceland. A cursory examination of the mechanisms of foreshocks shows significant variation, and further work is needed to test whether they can provide additional constraints on the fault-slip direction in addition to the fault-strike and -dip.

References

Clifton, A. E. & Einarsson, P. (2005). Styles of surface rupture accompanying the June 17 and 21, 2000 earthquakes in the South Iceland Seismic Zone. *Tectonophysics* 396, 141-159.

Hjaltadóttir, S. & Vogfjörd, K. S. (2005). Subsurface fault mapping in Southwest Iceland by relative location of aftershocks of the June 2000 earthquakes. *Icelandic Meteorological Office report*, VÍ-ES-01, Report no. 21.

Pétursson, G. G., Vogfjörd, K. S. & Ágústsson, K. (2008). Attenuation relations for near-field and far-field peak ground motion and new magnitude estimates for large earthquakes in Iceland, *SAFER deliverable D5.2* and manuscript in preparation.

Slunga, R., Rögnvaldsson, S. Th. & Bödvarsson, R. (1995). Absolute and relative locations of similar events with application to microearthquakes in southern Iceland *Geophys. J. Int.*, **123**, 409-419.

Stefánsson, R., Gudmundsson, G. B., Halldórsson, P. (2000). The two large earthquakes in the South Iceland seismic zone on June 17 and 21, 2000. *Icelandic Meteorological Office report,* VÍ-G00010-JA04.

Vogfjörd, K. S., Pétursson, G. G., Kjartansson, E., Slunga, R., Ágústsson, K., Hjaltadóttir, S., Gudmundsson, G. B., Roberts, M. J., Geirsson, H. & Ármannsdóttir, S. (2008). Seismic and tsunami early warning activities in Iceland. EGU spring meeting in Vienna, 13-18 April 2008, *Geophysical Research Abstracts*, Volume10, 11538.

Project no. **036935**

Project acronym: **SAFER**

Project title: **Seismic eArly warning For EuRope**

Instrument : **Specific Targeted Research Project**

Thematic Priority: **Sustainable development, global change and ecosystem priority**
6.3.iv.2.1: Reduction of seismic risks

D2.29 Implementation of real-time fault mapping in SW-Iceland

Sigurlaug Hjaltadóttir,[1)] Gunnar B. Gudmundsson,[1)] Kristín S. Vogfjörd,[1)] and Ragnar Slunga[2)]
[1)] Icelandic Meteorological Office
[2)]QuakeLook AB Stockholm

Implementation of real-time fault mapping in SW-Iceland

Introduction

Fast determination of earthquake mechanism of major earthquakes enables quick estimation of the spatial distribution of shaking caused by the event, and together with the magnitude estimate, provides important information for civil protection and disaster response teams in the first minutes following the earthquake. Foreshock distribution on the fault plane of an on-coming major event can potentially be used to define the fault's strike and dip, which can then be immediately assigned to the event when it occurs. For this to work, the foreshocks need to be numerous enough to constrain the fault plane and their location also needs to be quickly determined with high accuracy. This approach to fast initial estimate of mechanism has been taken for the SAFER region in SW-Iceland, where large earthquakes of magnitudes up to M7 have repeatedly occurred over the last millennium. The seismicity is a result of plate spreading at the Mid-Atlantic rift, which crosses Iceland from SW to NE. The rift runs along Reykjanes Peninsula (RP in Figure 1) towards the Hengill region (within the grey box of Figure 1), where the rifting is shifted ~100 km eastward along the South Iceland Seismic Zone (SISZ), a left-lateral shear zone characterized by parallel, N-S oriented, vertical strike-slip faults. In the last 19 years of SIL network operation, over 130 thousand microearthquakes have been recorded in southwest Iceland, and in the last nine years, three M>6 and six M>5 events have occurred in the SISZ and Reykjanes peninsula (stars in Figure 1).

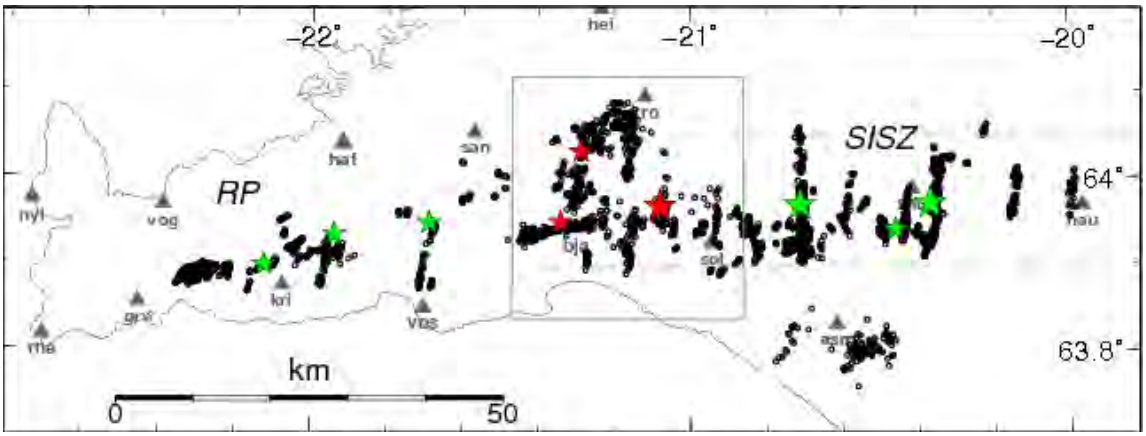

Figure 1. A map of south-west Iceland showing Reykjanes Peninsula (RP), the Hengill-Ölfus area (within box) and the South Iceland Seismic Zone (SISZ, within dashed region). Library events on previously mapped faults in SW-Iceland are shown in black. Grey triangles denote SIL seismic stations. Large green stars show location of the two M~6.5 events in June 2000. The four smaller green stars show the location of four M>5 events that occurred minutes after the first (easternmost) large event in 2000. Small red stars show location of two M>5 earthquakes in the Hengill-Ölfus area in 1998 and the large red star shows the initiation of rupture on the eastern fault of the M6.3 earthquake in Ölfus in May 2008.

The fault planes of the main events in SW-Iceland have been mapped through relative relocation of their aftershocks, and fault planes of other historic earthquakes have similarly been mapped with the microearthquakes recorded by the network. The method used for relocation is the double-difference method of Slunga et al. (1995), which employs cross correlation of similar waveforms to improve the accuracy of relative time differences of the events, taking advantage of the high clock accuracy (1 ms) and sampling frequency (100 Hz) of the SIL network. Subsequent inversion of the relative time differences returns high-precision relative locations that enable resolution of faults and fault patterns. A selection of the best relatively located events in southwest Iceland is shown in Figure 1, where the traces of several fault planes are clearly outlined.

Method and Application

The idea is to use the thousands of previously relatively located events in southwest Iceland to enable fast and automatic high-precision locations of new events, in order to map the active fault planes in near-real time. For that purpose, an event library has been constructed containing a selection of well distributed events, previously relatively located, and with high location accuracy. The library contains representative events from each fault already mapped. Waveforms from the library events will be used to correlate with new events satisfying certain quality criteria. The new events, automatically detected and located by the SIL system, are available approximately 2 minutes after the origin time, but their location accuracy is sometimes low and does not warrant mapping of common faults. By correlating the waveforms from a new event with the waveforms of selected near-by events from the library and inverting for best location, the location accuracy can be substantially improved. The procedure has already been tested in three different source regions, returning accurate locations within minutes, as reported in D2.27. The process can start for each qualifying new event, as soon as waveforms from two stations have arrived and subsequently repeated as more waveforms become available.

As was demonstrated by the 29 May 2008, M 6.3 earthquake in the Ölfus district in the South Iceland Seismic Zone (SISZ), the use of foreshocks in this manner can work. The earthquake ruptured two faults, 4 km apart, with rupture initiating on the eastern, Ingólfsfjall fault (large red star in Figure 1, while slip on the second, Kross fault was triggered a few seconds later. The Kross fault can be seen in Figure 1. It is composed of two en echelons, approximately N-S oriented faults, 4 km west of the Ingólfsfjall fault (Vogfjörd et al., 2009). In the hour preceding rupture initiation of the main event, 40 foreshocks were recorded at the southern end of the Ingólfsfjall fault. Taking into account that it can take up to 10 to 15 minutes for enough waveforms to arrive at the data center to allow relative location of an event, the 25 foreshocks that had already occurred 15 minutes before the main event were relatively relocated with events from the library set. The distribution of the 25 events is shown in Figure 2. The events delineate a ~700 m long and 1.5 km wide fault plane which strikes N5°E and dips 89°. The strike deviates only 4° from the strike defined by the relocated aftershock distribution on the Ingólfsfjall fault, which shows an 11 km long and an 8 km deep fault, striking N181°E and dipping 89°. The mechanism of the earthquake on the Ingólfsfjall fault could therefore have been immediately inferred. However, there were only three foreshocks

on the (second) Kross fault during the 12 hours preceding the earthquake, so its fault plane could not have been envisaged with this method.

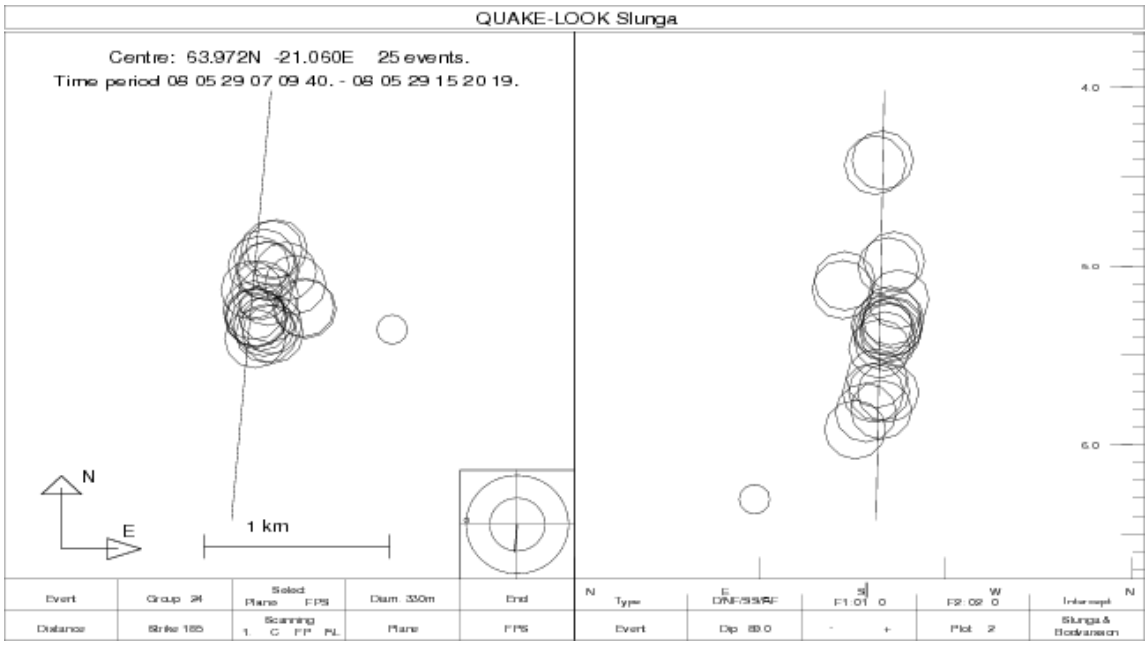

Figure 2. (Left) Map view of the foreshock distribution on the Ingólfsfjall (eastern) fault of the 29 May 2008 Mw6.3 earthquake; a total of 25 foreshocks occurring until 15 minutes before the large event. (Right) Vertical cross-section viewed from the north, showing the event distribution with depth. The events define a plane striking 5º and dipping 89º. The strike and dip of the plane are shown with a black line.

The near-real time relative location procedure has been automated and implemented in a test area of SW-Iceland. The test area includes the Hengill volcanic system and Ölfus district (grey boxed area in Figure 1). This area, in addition to the May 2008, M_w6.3 event, also experienced greatly increased seismic activity between 1994 and 1998, which ended with two, M5.5 and 5.2 earthquakes in 1998 (red stars in Figure 1). The region is well suited for testing since extensive fault mapping of the 1997-2008 seismicity has already been carried out (Vogfjörd et al., 2005) and aftershocks are still frequent on the faults that were active in 2008.

Details of the implemented procedure are as follows: A library of events on the previously mapped faults from 1997–1998 (pink in Figure 3), from 2000 (orange in Figure 3) and from 2008 (green in Figure 3) has been selected. When a new event with a quality above a certain limit (Q_{min}, in Table 1) is detected within the test area, library events within distance r are selected and stored in a temporary sub-library. If needed, the number of sub-library events is reduced to a maximum number (N_{max}) to limit processing time to a few minutes. Furthermore, if new events have been automatically relocated recently (D_{recent}), they are also added to the sub-library. The waveforms of the new event are then compared to the waveforms of the sub-library at stations within D_{max} distance. The 40 best correlating events are then chosen for inversion to obtain a relative location for the new event. The procedure is run every 5 minutes

(T_{int}) and is applied to events for which waveforms are available from at least S_{min} stations within distance D_{wf}. Table 1 describes various parameters in the automatic procedure.

Table 1. Values and description of parameters in the automatic procedure.

Parameter	Value	Description
Q_{min}	50 (10)	Required Minimum Quality of event
r	5 km	Distance from the automatic location, within which a sublibray is selected
N_{max}	200	maximum number of sub-library events
N_{min}	60 (100)	minimum number of sub-library events
D_{max}	70 km	Maximum distance from automatic location to station
S_{min}	2	Minimum number of stations used in relocation
T_{int}	5 minutes	Time between checking for new automatic events
N_{rec}	20	Maximum number of newly located events in a sub-library
T_{recent}	30 days	Recent time in days from which new events are added to the sub-library
D_{wf}	50 km	Distance limit of available waveforms from Smin

The procedure has been in operation since 26 May 2009, running automatically every 5 minutes looking for a new event in the area. When a maximum of 200 sub-library events is used, the processing time for each event is approximately 3-5 minutes. The map in Figure 2 shows automatic (yellow stars) and automatic relative locations (cyan) for approximately 100 events detected between 26 May and 11 June 2009, which also fulfilled the parameter criteria.

Expansion of the test area and future development

The first version of the software, running automatically in the Hengill-Ölfus test area, is still being tested and debugged and parameters are being tuned for optimum performance. When the testing and tuning has completed successfully, the process will be implemented for the whole target area in SW-Iceland. This is expected to take place in the fall of 2009. The library of events on previously mapped faults in the target area, from Reykjanes Peninsula through the length of the South Iceland Seismic Zone, has already been assembled. These events are plotted in Figure 1 and represent faults active following the two M~6.5 events in the SISZ in June 2000 (marked by large green stars in Figure 3) (Hjaltadóttir and Vogfjörd, 2005), faults on the Reykjanes Peninsula, active between 1997 and 2006 (Hjaltadóttir and Vogfjörd, 2006), as well as the fault of a M 4.6 earthquake near to the station **kri** in March 2006.

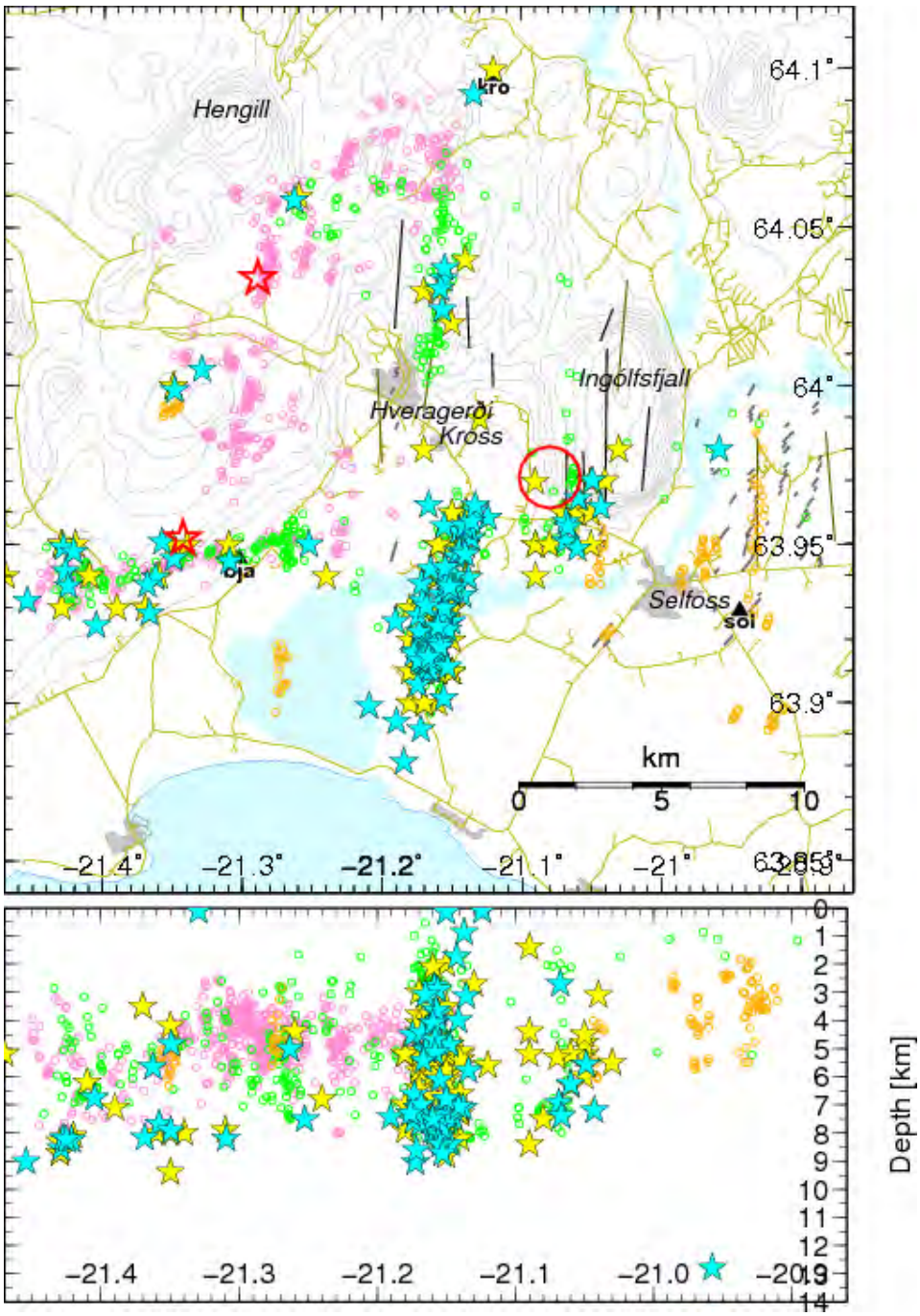

Figure 3. (Upper) A map showing the Hengill- and Ölfus test area. (Lower) A vertical cross section, viewed from the south. Pink circles show the 1997–98-library events, orange circles show library events from 2000 and green circles show 2008-library events. The red stars show location of two M>5 earthquakes in June and November 1998 and the red circle shows the location of the initial onset of the M 6.3 earthquake on 29 May 2008. Yellow stars show automatic locations for ~100 events which occurred between 26 May and 11 June 2009, and cyan stars show their automatic relative locations.

Further development of the procedure will focus on shortening the execution time, possibly by running locations of different events in parallel. The repeat time will also be shortened from the present 5 minute interval. Further improvements may also involve returning the improved locations automatically into the manual location-and-phase-picking software, in order to reduce the manual phase picking time. With the addition of one or two phase picks, a well constrained focal mechanism can subsequently be obtained for each foreshock within a few additional minutes (focal mechanisms are routinely calculated for all located events). The mean slip direction can then be estimated for the foreshocks and in the event of a following large earthquake, its full focal mechanism can be immediately assumed from the foreshocks' location and slip distribution.

When completed, the process is also expected to provide valuable input to improve shake-maps generated for large earthquakes – automatic generation of shake maps was developed under WP4. Fast, automatic relocation of aftershocks following a significant earthquake will then be used to delineate and map the full extent of the main events fault plane, and the fault dimensions subsequently input into the shake map, in order to improve the mapping of shaking intensity.

References

Hjaltadóttir, S. & Vogfjörd, K. S. (2005). Subsurface fault mapping in Southwest Iceland by relative location of aftershocks of the June 2000 earthquakes. *Icelandic Meteorological Office Report, Rit 21,* VÍ-ES-01.

Hjaltadóttir. S. & Vogfjörd, K. S. (2006). Mapping of faults at Fagradalsfjall on Reykjanes Peninsula (in Icelandic: Kortlagning sprungna í Fagradalsfjalli á Reykjanessskaga með smáskjálftum. Kortlagning jarðhita í gosbeltum Íslands – fyrsti áfangi). *Icelandic Meteorological Office Report,* nr. 06001, VÍ-ES-01.

Slunga, R., Rögnvaldsson, S. Th. & Bödvarsson, R. (1995). Absolute and relative locations of similar events with application to microearthquakes in southern Iceland. *Geophys. J. Int*., 123, 409-419.

Vogfjörd, K. S., Hjaltadóttir, S. & Slunga, R. (2005). Volcano-tectonic Interaction in the Hengill Region, Iceland during 1993-1998. *Geophysical Research Abstracts,* 7, 09947.

Vogfjörd, K. S., Hjaltadóttir, S., Geirsson, H., Gudmundsson, G. B. & Slunga, R. (2009). Fault interaction in the South Iceland Seismic Zone: The May 2008 M6.3 earthquake. *Geophysical Research Abstracts*, 11, EGU-2009-11748.

2. Real time estimation of earthquake magnitudes based on dominant frequency in P waves (*ElarmS*)

Project no. **036935**

Project acronym: **SAFER**

Project title: **Seismic eArly warning For EuRope**

Instrument : **Specific Targeted Research Project**

Thematic Priority: **Sustainable development, global change and ecosystem priority 6.3.iv.2.1: Reduction of seismic risks**

D2.28 Results of the effectiveness of IMO's version of the ElarmS method when applied to Iceland, and implementation of a version of ElarmS in Iceland

Kristín S. Vogfjörd and Einar Kjartansson
Icelandic Meteorological Office

Results on the effectiveness of the ElarmS method when applied to Iceland, and implementation of a version of ElarmS in Iceland

Introduction

Fast determination of magnitude of major earthquakes is an integral part of seismic early warning, because real-time processing – in matter of seconds – of information carried by the P-waves radiating from an earthquake can under certain conditions enable preventive measures to be taken, before the shear waves and surface waves arrive at a site. This requires that seismic stations be located near the epicenter and that the information processed and transmitted immediately. IMO's initial plan for incorporating such a process in the seismic monitoring in Iceland was through implementation of a modified version of the ElarmS code of Allen and Kanamori (2003) at the seismic stations of the SIL national seismic network. Work towards this goal, however, started late in the project, after a real-time process, estimating peak ground velocity and acceleration had already been developed and implemented at most of the network sites. Therefore it was decided to change the plan and add software to the existing driver, to enable real-time estimation of dominant period in P-waves along the lines of ElarmS.

The closeness of the capital, Reykjavík, where the majority of the Icelandic population resides, to the South Iceland Seismic Zone (40–70 km), where earthquakes of magnitudes 6 to 7 have repeatedly occurred over the last several centuries, precludes the capability for warnings to be issued or actions taken before damaging waves arrive in the capital. However, an operational and accurate on-line ElarmS algorithm can immediately – while the earthquake is still on-going at the capital – provide civil defence and response teams with the necessary information to assess the extent of possible damage or loss.

Method and Application

The real-time process developed and implemented in WP4 at all stations of the SIL network, monitors velocity and acceleration in a range of pass bands appropriate for magnitudes in the range $1.5 < M < 7$. Its purpose is to determine PGV and PGA in the S-wave window from events exceeding a background reference level. When the level is exceeded, the station sends a report to the data center. The process also attempts to solve for location and if successful, calculates magnitude using the attenuation relations describing the decay of PGV with distance, which were developed in WP5 and described in D5.2 (Pétursson and Vogfjörd, 2009). These are then prerequisites for the generation of ShakeMap.

To this process a new driver was added, which extracts the dominant period, τ_{max} in an event's P-wave, and then uses the τ_{max} estimate to determine the event magnitude. To estimate the dominant period, τ_{max} the new driver monitors the spectral ratio between band-pass filtered velocity and acceleration during the first 4 seconds after triggering. In the first 1-2 seconds of the P-arrival, the spectral division between the filtered velocity and acceleration records can be unstable. To stabilize the estimate, τ_{max} is determined from the maximum value attained in

the latter half of the time window; between 2 and 4 seconds after the trigger time. The value is immediately transmitted to the data center. The pass-band is within 0.075 to 3 Hz and is applied to both velocity and acceleration records, whereas in ElarmS the acceleration record is only low-pass filtered (Allen and Kanamori, 2003; Shieh et al., 2008). The process was implemented on 9 stations of the SIL seismic network at month 36 (see Figure 1). The SIL network consists mostly of combinations of short-period sensors and digitizers, which prevents the ability to extract a reliable magnitude estimate for large events. The process will therefore only be installed at stations with broad-band or intermediate instruments. The nine stations already equipped with the new driver possess Guralp DM24 flat-response digitizers and either Lennartz velocity sensors, having a high-pass corner at 0.2 Hz or Guralp 3ESP broad-band sensors, with corners at 0.033 Hz. Three additional stations are equipped with broad-band sensors and several more have the Lennartz 5s + DM24 combination installed. These stations will be running the τ_{max} driver within the coming months.

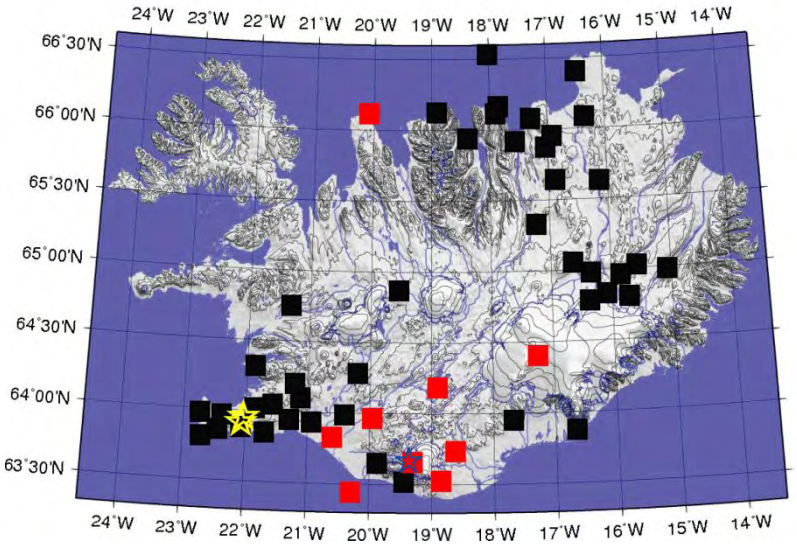

Figure 1. A map of Iceland showing the locations of the seismic stations of the SIL network (black squares). The nine stations where an ElarmS-type driver has been installed are coloured red. The two source regions of the four events on Reykjanes peninsula, returning reliable data from the ElarmS driver are marked with yellow stars. The location of Katla volcano is shown by a blue star.

The driver has been operational at the nine stations for a month and has returned one or more τ_{max} estimates from 16 local events, two regional events and one teleseismic event; a total of 76 estimates of τ_{max}. Of these 19 events, four local events on Reykjanes peninsula (yellow stars in Figure 1), in the magnitude range 3.3–4.2 have provided reliable estimates of dominant period, consistent between stations and events (see Figure 2). The estimates from a M5.4 event at 15º distance in Svalbard are contaminated by S-waves, because the driver did not trigger on the first P-arrivals. However, P-waves from a magnitude 6.0 event in Baffin Bay, at 21º distance triggered the driver at four of the stations, returning estimates which are

considered reliable. The two estimates from a M6.4 event in Crete, at 40º distance are probably also rather good.

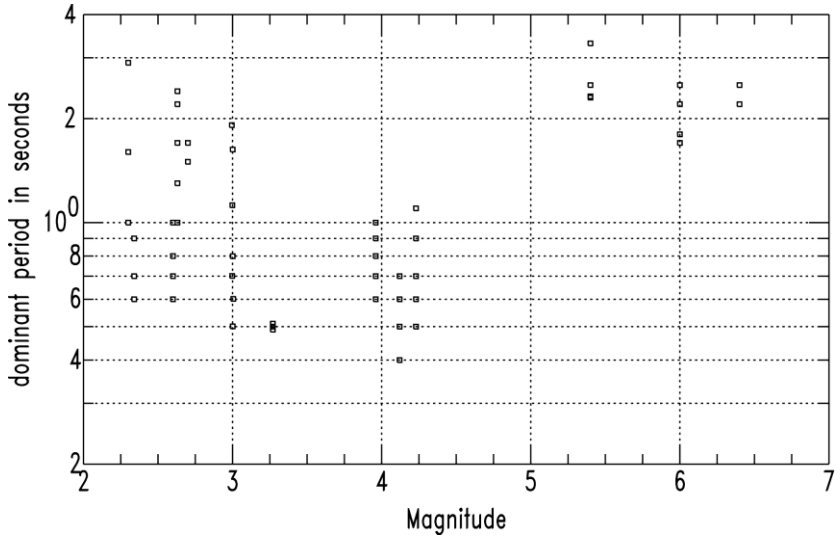

Figure 2. Dominant period, τmax of P-waves as a function of magnitude in 19 earthquakes generating reports from the stations equipped with the software. The four events on Reykjanes peninsula generated the estimates between 3.3<M<4.5. These are the most reliable estimates. The three largest events are in Svalbard (M5.4), Baffin Bay (M6.0) and Crete (M6.4). The high values τmax at magnitudes below M3 are generated by the LP events in the Katla volcano.

The algorithm does not handle events smaller than M3 very well; they usually trigger only one or two stations and the estimates obtained are rather scattered. The long-period M2-3 events constantly occurring in the Katla volcano in southern Iceland (shown with a blue star in Figure 1) are also problematic. They have very different characteristics from regular tectonic events in Iceland and return very high τ_{max} values, corresponding to magnitudes around M5. Estimates from four such events are included in Figure 2 (at M=2.3, 2.6, 2.7 and 3.0). Discriminating the LP Katla events from actual large events will be problematic.

Future development

In about a year of operation, the process is expected to have provided numerous enough estimates from a wide enough magnitude range to allow estimating a relationship between magnitude and dominant period, similar to estimates obtained in California (Wurman et al., 2007). Then it will be possible to determine whether a robust relationship between dominant period, τ_{max} and magnitude can be defined and used to return real-time estimates of event magnitude within 4+ seconds of recording. If such a relationship can be established, the process to manipulate the τ_{max} data at the center will be constructed. As the present algorithm is installed on more stations in northern Iceland, it will become useful in seismic early warning, and possibly even early warning for wave phenomena (tsunami) generated by large earthquakes in the Tjörnes Fracture Zone, off-shore northern Iceland.

References

Allen, R. M. & Kanamori, H. (2003). The potential for earthquake early warning in southern California, *Science*, 300, 786-789.

Shieh, J-T.,Wu, Y-M. & Allen, R. M. (2008). A comparison of τ_c and τ^p_{max} for magnitude estimation in earthquake early warning. *Geophys. Res. Lett*., **35**, L20301, doi:10.1029/2008GL035611.

Pétursson, G. G. & Vogfjörd, K. S. (2009). Attenuation relations for near- and far-field peak ground motion (PGV, PGA) and new magnitude estimates for large earthquakes in SW-Iceland. Icelandic meteorological Office Report (in preparation).

Wurman, G., Allen, R. M. & Lombard, P. (2007). Toward earthquake early warning in northern California. *J. Geophys. Res*., 112, B08311, doi:10.1029/2006JB004830.

3. Intensity vs. peak ground acceleration (PGA) and peak ground velocity (PGV) in SW-Iceland

Project no. **036935**

Project acronym: **SAFER**

Project title: **Seismic eArly warning For EuRope**

Instrument : **Specific Targeted Research Project**

Thematic Priority: S**ustainable development, global change and ecosystem priority 6.3.iv.2.1: Reduction of seismic risks**

D4.34 Intensity vs. peak ground acceleration and peak ground velocity in SW-Iceland

Páll Halldórsson and Kristín S. Vogfjörd
Icelandic Meteorological Office

Intensity vs. peak ground acceleration and peak ground velocity in SW-Iceland

Introduction

This report summarises the results of a study of the relationship between felt intensity in Icelandic earthquakes and measurements of peak ground acceleration (PGA) and peak ground velocity (PGV). The relationship is necessary input for Shake Map, which will be installed in SW-Iceland under SAFER's WP4. The relation is derived from reports of felt intensity and velocity and acceleration measurements in the five earthquakes listed in Table 1.

Table 1. Earthquakes used in the study.

Date of Earthquake	Location		Magnitude M_{Lw}
	Lat (°N)	Lon. (°W)	
04.06.1998	64.04	21.29	5.0
13.11.1998	63.95	21.35	4.8
17.06.2000	63.97	20.37	6.6
21.06.2000	63.87	20.07	6.6
23.08.2003	63.90	22.09	5.0

Data Analysis

The PGV, and PGA values from the earthquakes were obtained from deliverable D5.2, based on 3-component velocity data from the national digital seismic network SIL operated by Icelandic Meteorological Office (Pétursson et al., 2008). The 18 stations used provided 25 observations. The stations are all located in southern Iceland, at distances within 215 km from the epicenters. In addition PGA and PGV values were obtained from acceleration data from 17 stations in the Icelandic Strong Motion Network operated by the Earthquake Engineering Research Centre (available at: www.isesd.hi.is). These stations provided 45 observations at distances within 95 km. Locations of earthquakes and stations are shown in Figure 1.

All five earthquakes are located in SW-Iceland. The two largest are in the South Iceland Seismic Zone (SISZ), two are at the intersection of the SISZ with the Western Volcanic Zone (WVZ) and one is farther west in the WVZ, on Reykjanes Peninsula. While the SISZ region is rather densely populated farmland, with a few small villages, the WVZ is mostly uninhabited, but close to several villages as well as to the capital Reykjavík and its suburbs. The felt intensity reports are much more numerous than the velocity and acceleration measurements, but the reports very rarely occur at the observation sites. Therefore intensity reports from areas within 10 km of the stations were collected and analysed and used to

represent the observation site. The number of reports used for each earthquake, as well as their division into intensity classes is shown in Table 2.

Surface layers in the region where the earthquakes were felt consist mostly of young rock formations dating from the last glaciation or younger. The relations derived may therefore not apply to sites on older rock. It is, however, not clear what the difference would be, if any.

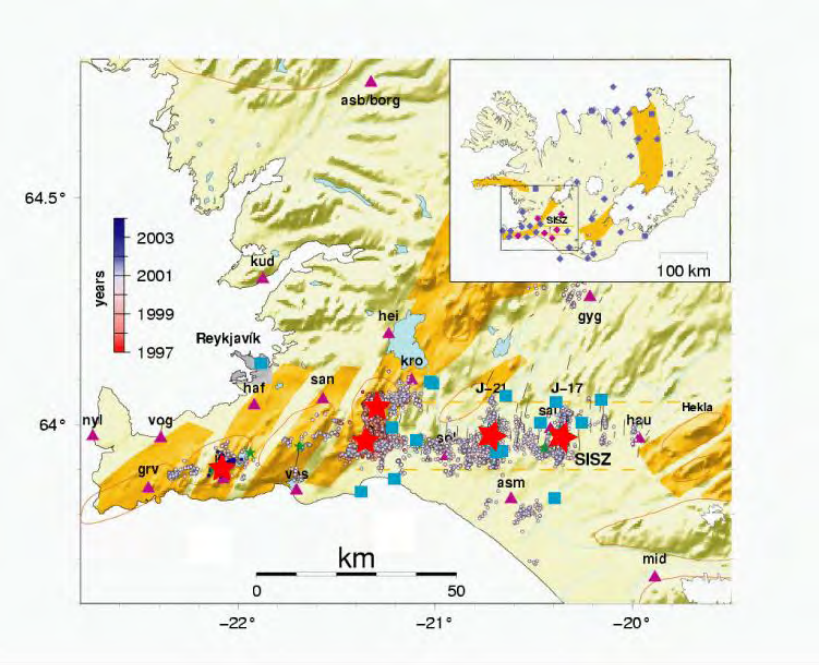

Figure 1. Map of SW-Iceland showing earthquake locations (red stars), locations of stations in the SIL seismic network (purple triangles) and of stations in the strong-motion network (blue squares). The volcanic zones are shown in orange and the South Iceland Seismic Zone is outlined with dashed orange lines. The coloured dots represent mapped earthquakes during 1997–2000.

Table 2. Number of intensity reports with respect to earthquake and intensity level.

		Intensity					
		IV	**V**	**VI**	**VII**	**VIII**	**Total**
Earthquake	04.06.1998	9	4	1			14
	13.11.1998	1	3	1			5
	17.06.2000	2	11	2	4		19
	21.06.2000	3	9	8		3	23
	23.08.2003	7	2				9
	Total	**22**	**29**	**12**	**4**	**3**	**70**

.

Table 2 shows that the number of reports of felt intensity decreases with intensity level and that only in the two earthquakes whose magnitudes are larger than 6 were intensity levels VII and VIII reached. The fact that no level VII intensity was felt for the of 21 June 2000 earthquake and no level VIII for the 17 June 2000 earthquake, is a mere coincidence. Intensity levels VII and VIII were felt at other locations in both of these earthquakes. The intensity as a function of PGV is shown in Figure 2, and as a function of PGA in Figure 3. The relationships between the logarithm of the PGV and PGA values and the intensity values were estimated with linear least-squares, but due to the scarcity of data for the higher intensity levels the curve was fitted to the average of each intensity level.

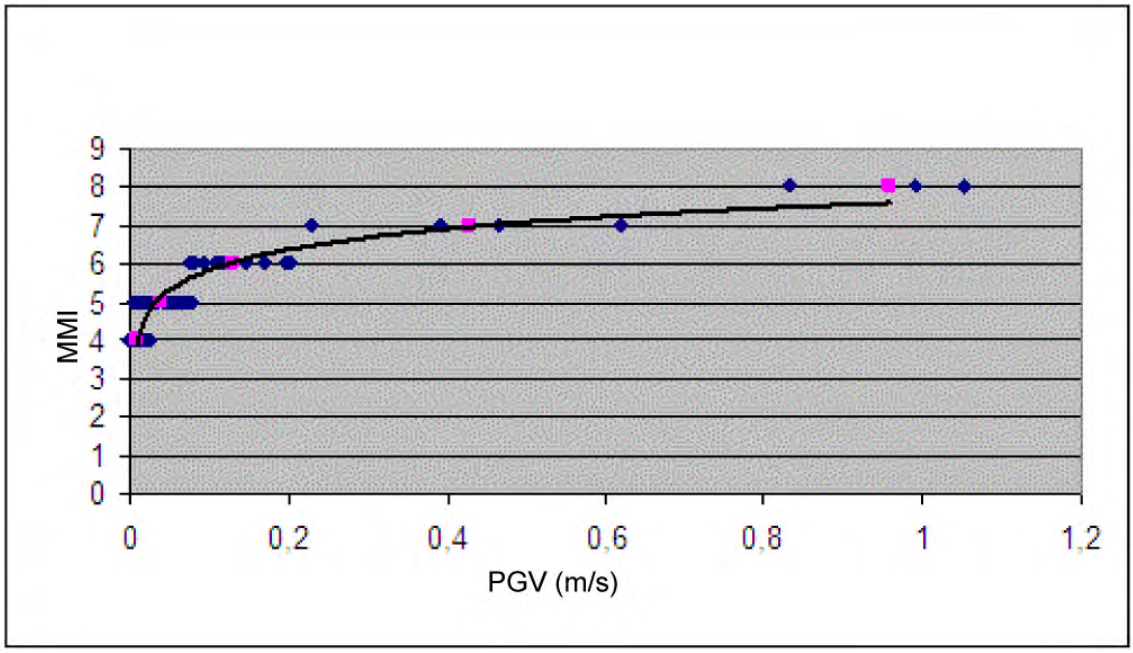

Figure 2. Intensity values as a function of peak ground velocity (PGV). The curve is fitted to the average values (pink) at each intensity level.

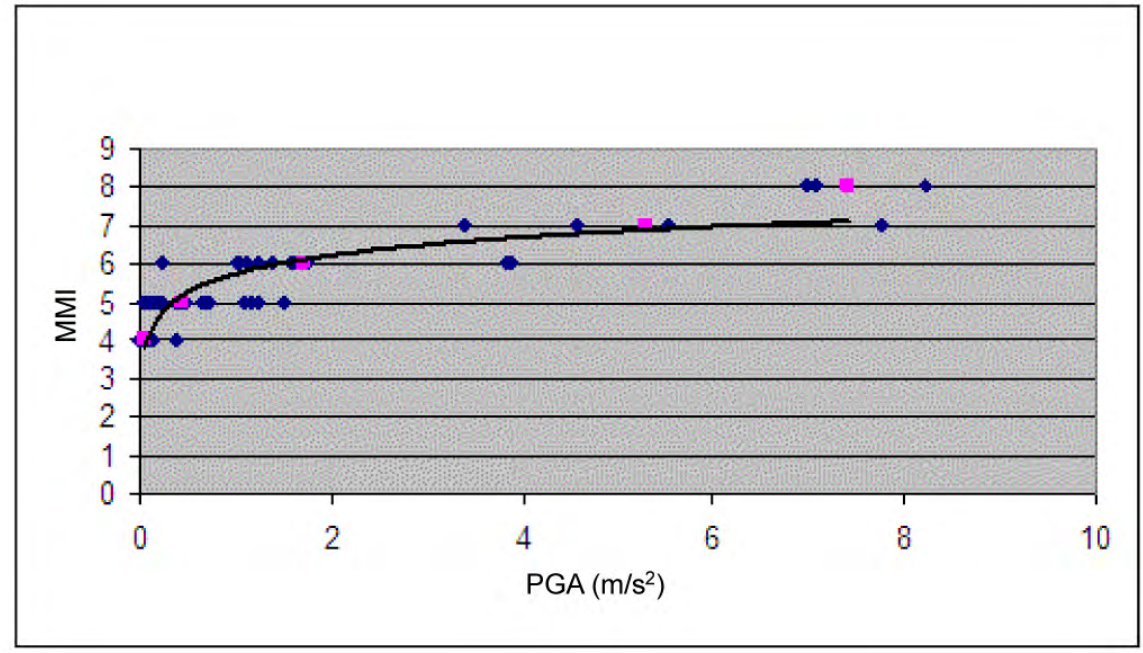

Figure 3. Intensity values as a function of peak ground acceleration (PGA). The curve is fitted to the average values (pink) at each intensity level.

The best fitting curve through the velocity dataset is given by:

$$MMI = 1.9 \log_{10}(PGV) + 7.7$$

The relationship between intensity and peak ground acceleration, derived in the same manner is given by:

$$MMI = 1.6 \log_{10}(PGA) + 5.7$$

The above equations were used to generate a table showing the PGV and PGA ranges corresponding to each intensity level between IV and VIII, such as is the custom in Shake Map, where for example the PGV and PGA ranges corresponding to intensities between 3.5 and 4.5 are taken to represent intensity IV and so forth. These values are shown in Table 3. For comparison, values from Wald et al. (1999) for California are also included in the table.

Table 3. (left) Peak ground velocity ranges corresponding to intensity levels IV to VIII. (right) Peak ground acceleration ranges corresponding to the same intensity levels. Californian values are from Wald et al., 1999.

MMI	PGV in SW-Iceland	Min	Max	PGA in SW-Iceland	Min	Max
IV	m/sec	0.006	0.021	m/sec^2	0.042	0.178
	cm/sec	0.6	2.1	% g	0.4	1.75
	California (cm/sec)	1.1	3.4	California (%g)	1.4	3.9
V	m/sec	0.021	0.070	m/sec^2	0.178	0.750
	cm/sec	2.1	7.0	% g	1.75	7.36
	California (cm/sec)	3.4	8.1	California (%g)	3.9	9.2
VI	m/sec	0.070	0.23	m/sec^2	0.750	3.16
	cm/sec	7.0	23	% g	7.36	31.0
	California (cm/sec)	8.1	16	California (%g)	9.2	18
VII	m/sec	0.23	0.78	m/sec^2	3.16	13.3
	cm/sec	23	78	% g	31.0	130
	California (cm/sec)	16	31	California (%g)	18	34
VIII	m/sec	0.78	2.64	m/sec^2	13.3	(56.2)
	cm/sec	78	264	% g	130	(551)
	California (cm/sec)	31	60	California (%g)	34	65

Table 3 shows that the PGV and PGA values in SW-Iceland increase faster with increasing intensity than is the case for California. However, for intensity levels IV to VI, the Icelandic values agree fairly well with the Californian values. Above that the Icelandic values are much higher. Table 2 and Figures 2 and 3 show that the values for intensities VII and greater are based on very few observations and may therefore be less reliable.

Summary

Relations between intensity, PGV and PGA were determined from 90 observations of velocity and acceleration and felt reports from five earthquakes in SW-Iceland. The relations were then used to calculate the PGV and PGA ranges corresponding to each intensity level, such as is the custom in Shake Map displays. The PGV and PGA values for intensity levels ranging from IV to VI are in fair agreement with Californian values (Wald et al., 1999), but are much higher for greater intensities. Scarcity of data for intensities above VI may affect the reliability of the results for these greater intensities.

It is interesting to note that no intensities greater than VIII were reported for any of the five earthquakes. The reason may lie in the way the intensity information was gathered. The questionnaires sent out following the earthquakes focused mainly on the effects experienced by people, or observations of moving objects, but to a lesser degree on the observed effects on buildings and structures. However, as intensity increases above VIII, the number of reports on how people experience an earthquake decreases. The limitations of the questionnaires are partly due to the fact that they have always been based on a Modified Mercalli Intensity scale from 1931, in which descriptions of damages to houses and other structures are of limited use when applied to Icelandic houses.

Acknowledgements

We thank G. G. Pétursson for assistance with translation of the initial Icelandic text. Map in Figure 1 was made with the GMT software.

References

Pétursson, G. G., Vogfjörd, K. S. & Ágústsson, K. (2008). Attenuation relations for near-field and far-field peak ground motion an new magnitude estimates for large earthquakes in SW-Iceland, *SAFER deliverable D5.2* and manuscript in preparation.

Wald, J., Quitoriano, V., Heaton, T. H. & Kanamori, H. (1999). Relationships between peak ground acceleration, peak ground velocity, and modified Mercalli intensity in California, *Earthquake spectra*, 15(3), 557-465.

4. Development of automatic real time "alert maps" maps and shake maps (ShakeMap) for earthquakes in SW-Iceland

Project no. **036935**

Project acronym: **SAFER**

Project title: **Seismic eArly warning For EuRope**

Instrument : **Specific Targeted Research Project**

Thematic Priority: **Sustainable development, global change and ecosystem priority 6.3.iv.2.1: Reduction of seismic risks**

D4.35 Analysis of the applicability of using station alerts for the purpose of generating "alert maps" within minutes of a large earthquake in SW-Iceland

Einar Kjartansson, Steinunn S. Jakobsdóttir and Kristín S. Vogfjörd
Icelandic Meteorological Office

Analysis of the applicability of using station alerts for the purpose of generating "alert maps" within minutes of a large earthquake in SW-Iceland

The SIL seismic network in Iceland consists of, at end of 2007, 51 seismic stations located in the most seismically active regions of Iceland; each station includes a computer running a Linux operating system (Redhat 7.3 in most cases). The stations are linked to the processing centre at IMO via various methods. Parametric information is sent automatically from the stations to the centre, but waveform data are only sent upon request. Parameter data, such as arrival times and amplitudes of P- and S-phases detected at the stations, are used at the centre to automatically locate and determine the magnitude of earthquakes. This process is usually quick, but can take a few minutes. Additional parameters are contained in a station alert log which is sent to the centre when the filtered signal at a station exceeds a predefined value. After an earthquake occurs, the station alerts are the first logs to be sent out and the first to arrive at the centre, usually a few seconds after generation. Currently they are used to alert the seismologist on duty of a possible impending event by activating the audio devices on the centre's workstations. We are interested in exploring the feasibility of utilizing the information carried by the station alerts more fully, by visually displaying the alerts in near-real time on a web-published alert map. When necessary, the information can then be immediately accessed by Civil Defence, the general public and other scientists.

The alert logs include the time when the threshold was exceeded and can possibly be used to infer the source region. They do not contain an accurate indication of peak values for the seismic signal, however, the extent of the region issuing station alerts is an indication of the magnitude of the event. In order to evaluate the suitability of the station alerts for early warning, in other words to indicate approximate event location, and to suggest the possible minimum magnitude before the earthquake has even been properly located, we have examined existing alert logs generated by three events: two events, located just east of lake Kleifarvatn on the Reykjanes Peninsula, and one event located at the village Selfoss in the South Iceland Seismic Zone. The events' source parameters are listed in the following table, where Mlw is a local magnitude based on the seismic moment of the event:

Date	**Latitude**	**Longitude**	**Depth**	**Magnitude**	
Aug. 23rd 2003	63.905°N	22.085°W	3.7 km	5.2(NEIS)	5.2(Mlw)
Mar. 6th 200663.	921°N21.9	22°W	8.1 km	4.2(NEIS)	4.6(Mlw)
Nov. 20th 2007	63.949°N	20.989°W	1.8 km		3.3(Mlw)

The first two events generated alert logs at most stations, but the third event at only two stations. Maps showing the times when the filtered signal at each station exceeded the thresholds were generated for the two larger events. Figure 1 shows the relative time when the

threshold was exceeded for the M5.2 event, and Figure 2 shows the time for the M4.2 event. Even though not all stations issued alerts, the location of both events can be easily inferred. Furthermore, both events generated station alerts at the most distant stations.

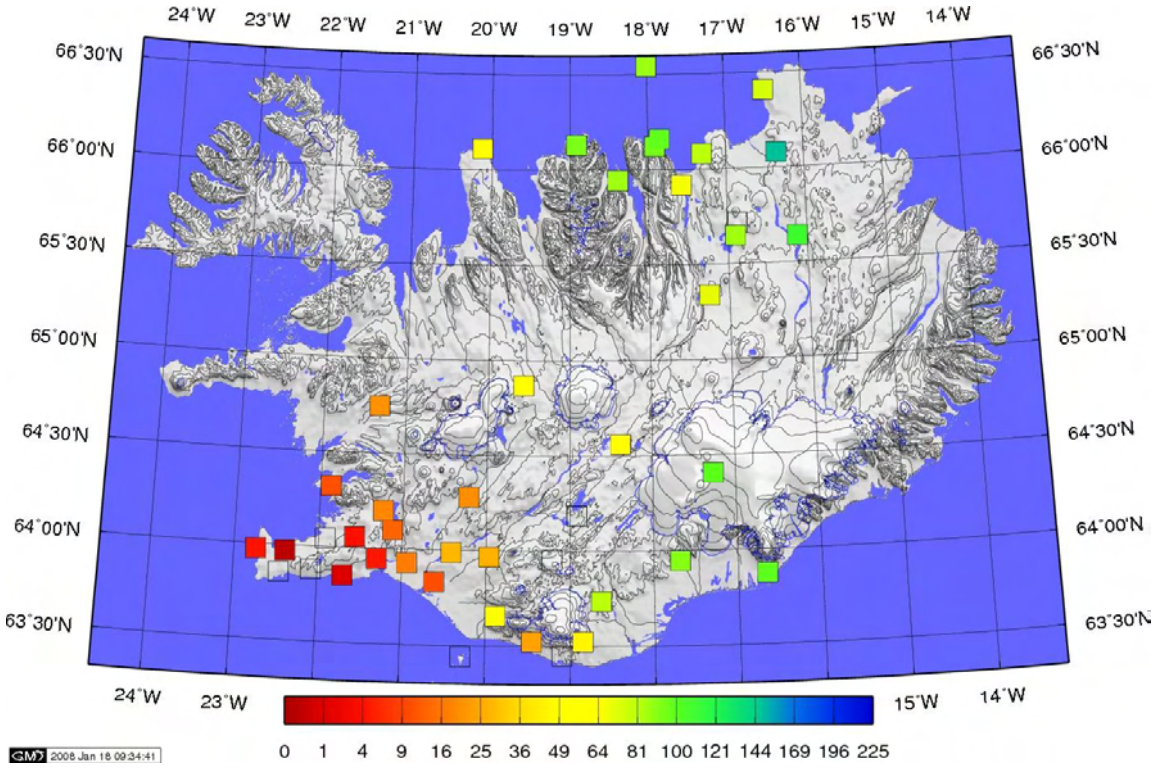

Figure 1 Relative time (seconds) of station alerts, indicated by coloured boxes, at seismic station locations across Iceland, for an M5.2 on August 23 2003 at 02:00:12. Transparent boxes indicate stations that did not issue alerts.

The results demonstrate that at least for events of M4 and greater, the present station alerts can be used as a basis for a useful early seismic warning tool. Considering the speed with which the alerts arrive at the centre, it should be possible within 30–40 seconds of an earthquake to generate, and make accessible on the web, maps showing relative times for stations within 100 km distance, thus giving an approximate location. In another minute, an estimate of the minimum magnitude can be made, based on the spatial extent of the alerts.

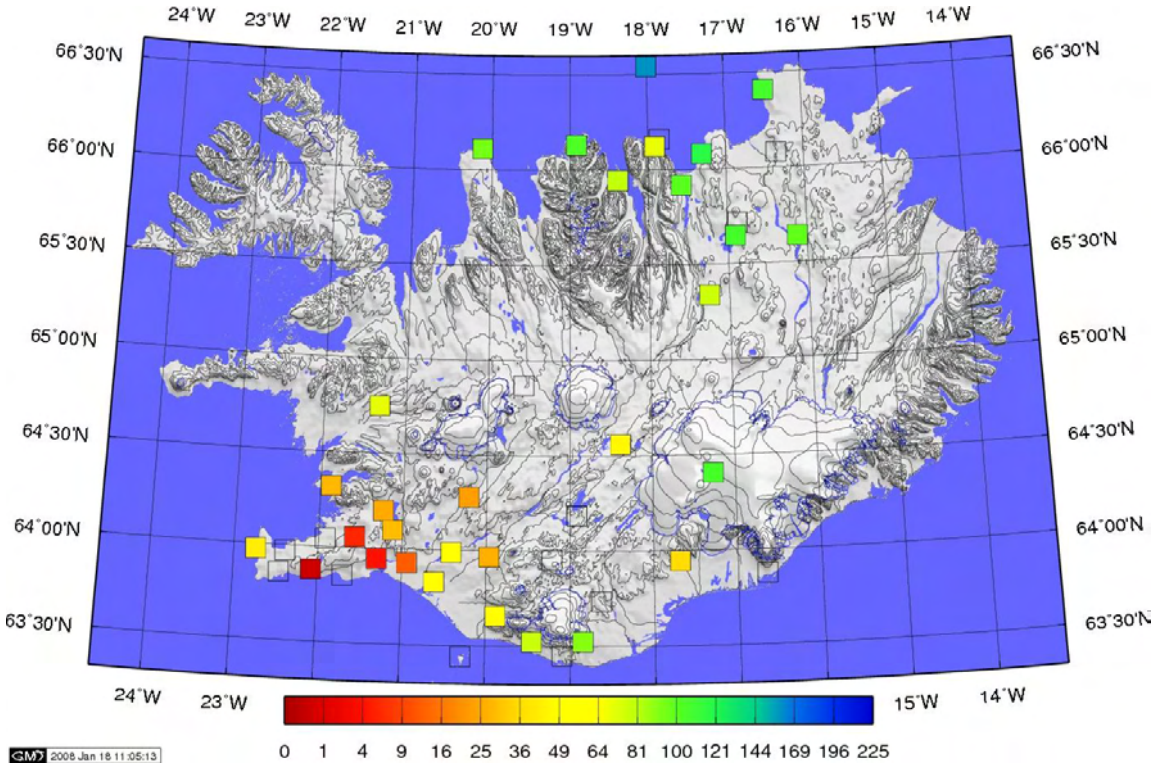

Figure 2 Relative time (seconds) of station alerts, indicated by coloured boxes, at seismic station locations across Iceland, for a M4.5 event on March 3rd 2006 at 14:31:55.

We plan to implement an automatic procedure to generate this kind of alert map for earthquakes in Iceland, using the threshold times contained in the present logs. We also plan to install software on the station computers with real-time filters and detectors that are specifically designed to provide seismic early warning. When this has been implemented, we expect to be able to produce alert maps for events with magnitudes of around 2.5, down from the M4 of the present software.

Project no. **036935**

Project acronym: **SAFER**

Project title: **Seismic eArly warning For EuRope**

Instrument: **Specific Targeted Research Project**

Thematic Priority: **Sustainable development, global change and ecosystem priority 6.3.iv.2.1: Reduction of seismic risks**

D4.36 Evaluation and development of a procedure for using phase-log data from seismic stations for automatic generation of shake maps on a 5x5 km grid, within minutes of large events in SW-Iceland

Einar Kjartansson, Hjörleifur Sveinbjörnsson, Kristín S. Vogfjörd, Sigthrúdur Ármannsdóttir and Bergthóra Thorbjarnardóttir
Icelandic Meteorological Office

Evaluation and development of a procedure for using data from seismic stations for automatic generation of shake maps on a 10x5 km grid, within minutes of large events in SW-Iceland

The initial plan for implementing ShakeMap in Iceland involved using phase-log data, transmitted in real-time from the seismic stations of the SIL network to the data center at the Icelandic Meteorological Office. The phase logs include time of phase detection, amplitude of the phase (on all 3 components of motion), the phase type, and noise level in the time window preceding the detection. The logs are used by the SIL system to automatically locate and estimate event magnitude in real time. The SIL software does an excellent job of detecting and locating microearthquakes. However, it is not optimized for reliable determination of magnitude for moderate and large events. After initial inspection of the phase logs generated by a few of the larger events it was therefore decided to develop new tools, designed to reliably detect and process events in the magnitude range from M1.5 to M7 and prepare the necessary data for the generation of alert maps and ShakeMaps. This new tool includes a range of pass bands appropriate for different magnitude ranges. Such a real-time analysis tool has been constructed and implemented at all 55 stations of the SIL network, with the final stations activated at month 35.

Table 1. Filters used in parallel real-time processing of seismic signals. The right column shows the approximate magnitudes corresponding to the lower corner frequencies of the filter pass bands. The lowest frequency filter is only used at stations with broadband sensors and only the two highest frequencies are used at stations with Lennartz 1Hz seismometers.

Pass band	Low corner	High corner	Magnitude
	(Hz)	(Hz)	
High	4	50	3.5
Medium	1	10	4.7
Low	0.25	2.5	5.9
Very low	0.05	0.5	7.1

The real-time process running on each station computer monitors both ground velocity and acceleration in 4 separate and overlapping frequency bands. The pass bands are listed in Table 1. A reference level is maintained for both horizontal and vertical components in each frequency band, chosen so that the level is exceeded a few times per hour. When signals exceed this reference level by more than 50% a report is sent from the station to the processing center. This ensures good sensitivity while keeping the number of false reports

down. When 5 or more stations send reports within a time interval of 20 seconds, an alert map is generated. The alert map, which can be ready on the web 1.5 minutes after origin time of the event, shows the observed values for each station. They are: time of first break, Peak ground velocity (PGV) and time of PGV. Heap data structures are used to find the PGV and PGA values within a symmetric time window in an efficient manner. The length of the window is chosen to be longer than the period corresponding to the lower frequency limit of the respective filter. The alert maps are immediately accessible on the web at the location: http://hraun.vedur.is/ja/alert. An example from a M4.7 event on Reykjanes peninsula on 29 May, 2009 is presented in Figure 1. The figure shows the time of first break and the PGV amplitude at reporting stations of the network and very clearly demonstrates the approximate event location. Implementation of the process at all network sites was finally completed in early June, 2009. Examples of a PGV alert map for a M4.2 event on June 19, 2009, where the whole network is contributing information is shown in Figure 2

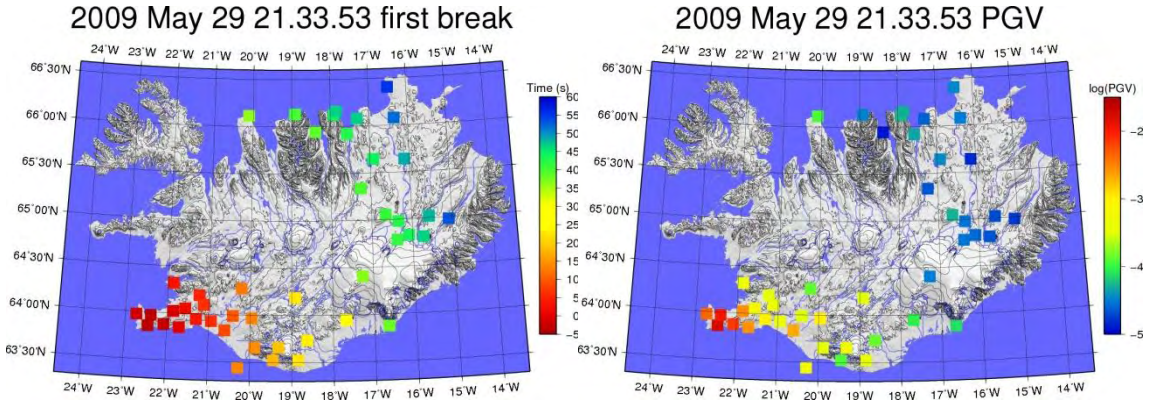

Figure 1. (Left) Time of first break in a M4.7 event on Reykjanes peninsula (RP) in SW-Iceland. The squares represent the seismic stations where the real-time alert process has been installed. The squares are colour coded according to the same reference time, with the time scale shown on the right. The earliest trigger times are on RP. (Right) Peak ground velocity (PGV) of the event in log(m/s), where the squares are colour coded according to PGV, shown on the scale to the right. The maximum PGV, (>1 cm/s) is observed on RP. The alert maps, available in 1.5 minutes, clearly show that the event origin is on Reykjanes peninsula and the felt shaking is confined to RP and vicinity.

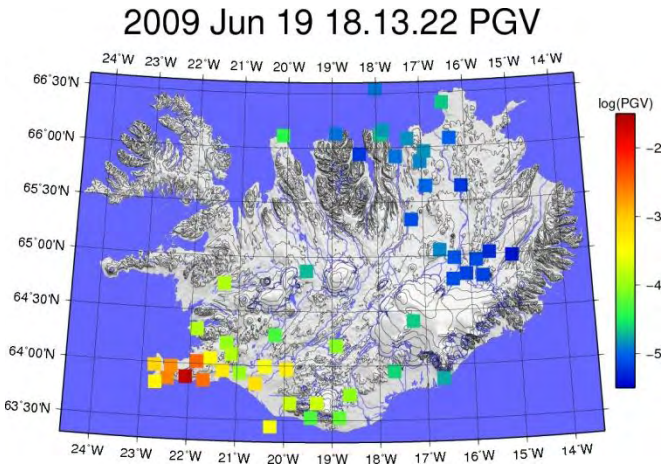

Figure 2. PGV values, in log(m/s) generated by an M4.2 event on June 19, 2009, when all stations of the SIL network had been equipped with the early warning alert process.

An attempt is also made to solve for the location and magnitude of the event. This is done by checking all trigger times for consistency of P-wave travel time, i.e. if the trigger-time difference between a station and its near-by stations is greater than the P-wave travel time between them, then the station is discarded. If four or more stations are still left after this process, then all possible combinations of 3 stations are used to compute potential solutions. The location that yields the lowest sum of absolute residuals for all remaining stations is then selected. Once the location has been determined, conventional magnitude is calculated using the attenuation relations describing the decay of PGV with distance (see D5.2, Pétursson and Vogfjörd, 2009). When a good fit is obtained for both arrival times and amplitudes at 5 or more stations, and the magnitude indicated is greater than 2.0, the location and magnitude information are placed on the web with the alert maps, and a ShakeMap is generated and placed online automatically.

The ShakeMap software uses the attenuation relations for PGV and PGA derived in D5.2 (Pétursson and Vogfjörd, 2009) as well as the relationships between Intensity and PGV and PGA derived in D4.35. A map where near-surface geology in southwest Iceland was categorized into 7 different units was compiled during reporting period 2. To translate the geologic map into a near-surface S-wave velocity (V_s^{30}) map, the generic V_s/V_p relationship of Chandler et al. (2005) was used together with available information on near surface P-wave velocities in Iceland, obtained from measurements in boreholes, in laboratory rock samples and from refraction profiles, as summarized by Gunnarsson et al. (2005). The V_s^{30} map is used by the ShakeMap software to represent site effects. The geological units and corresponding velocity estimates are listed in Table 2 and the map is shown in Figure 3. The velocities are considerably higher than those of the California site-category map constructed by Wills et al. (2000), and the near-surface velocities summarized by Chandler et al. (2005). The main reason for this difference may be that sedimentary layers are rare (and thin) in Iceland and significantly metamorphosed rocks are rarely found near the surface. The older, Tertiary rocks (green in Figure 3) are mostly glacially eroded lava flows and the younger formations in the rift zones (violet and brown in Figure 3) generally consist of fresh volcanics.

Table 2. Nine different categories used to describe the geological units in ShakeMap, and their corresponding shear-wave velocity estimates. Velocities of under-water (lakes, oceans) geological units are estimated.

Vs (km/s)	Geological Unit
0.60	Sediment, mostly alluvium, thickness greater than 30 m
0.70	Sediment, thickness less than 30 m
0.75	Lakes – unknown basement
0.80	Ocean – unknown basement
1.20	Hyaloclastite and rhyolite
1.30	Holocene lava, less than 25 m thick on top of sediments
1.50	Holocene lave
1.60	Basaltic lava, younger than 0.8 million years
2.00	Basalt, older than 0.8 million years

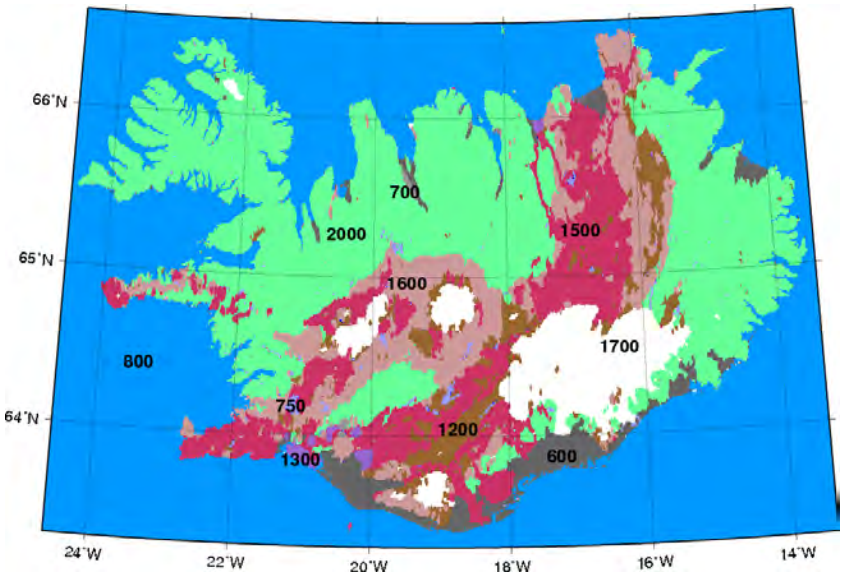

Figure 3. Near-surface geology of Iceland showing the nine categories of estimated V_s^{30} velocities. The units are described in Table 2.

The ShakeMap generated for the May 29, 2009 event on Reykjanes peninsula (corresponding to the alert maps in Figure 1) is shown in Figure 4. Compared to felt reports from the near-by town of Grindavík, 4 km to the south of the epicenter, the near-fault intensity may be slightly underestimated.

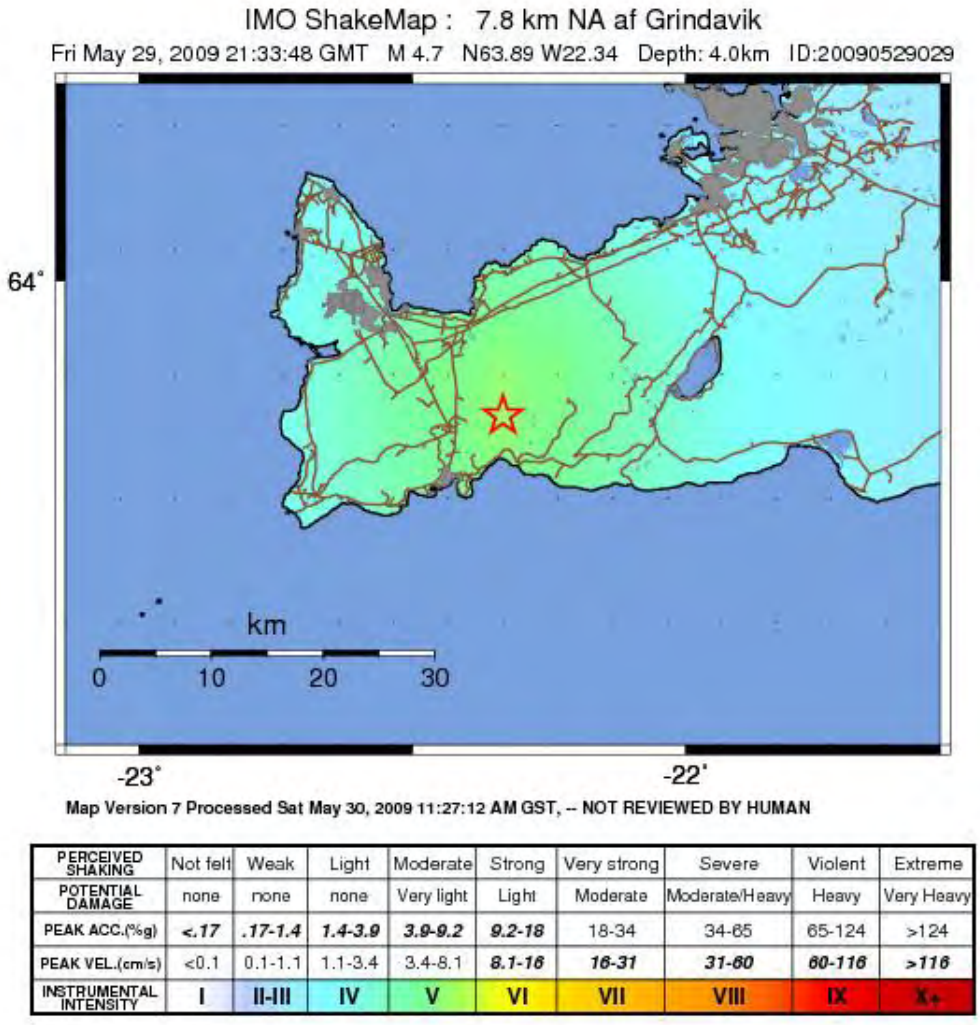

PERCEIVED SHAKING	Not felt	Weak	Light	Moderate	Strong	Very strong	Severe	Violent	Extreme
POTENTIAL DAMAGE	none	none	none	Very light	Light	Moderate	Moderate/Heavy	Heavy	Very Heavy
PEAK ACC.(%g)	*<.17*	*.17-1.4*	*1.4-3.9*	*3.9-9.2*	*9.2-18*	18-34	34-65	65-124	>124
PEAK VEL.(cm/s)	<0.1	0.1-1.1	1.1-3.4	3.4-8.1	*8.1-16*	*16-31*	*31-60*	*60-116*	*>116*
INSTRUMENTAL INTENSITY	I	II-III	IV	V	VI	VII	VIII	IX	X+

Figure 4. ShakeMap generated for the M4.7 earthquake on Reykjanes peninsula on May 29, 2009.

The ShakeMap is available 35 seconds after the alert map, or roughly 2 minutes after origin time of the earthquake and it can immediately be accessed at http://hraun.vedur.is/ja/alert. When information on the fault dimension becomes available – for example from the results of the automatic near-real-time relative-location of aftershocks, as described in D2.29 – the fault parameters can be incorporated to improve the ShakeMap. This has been done for the ShakeMap of 29 May, 2008 M6.3 earthquake near the town Selfoss in the South Iceland Seismic Zone (see Figure 5, left). The ShakeMap shows rather good agreement with felt intensity reports, which are shown on the right in Figure 5. The main discrepancy between the

two maps is in the near field of the two faults, where the ShakeMap underestimates the intensity. The difference is probably due to site effects not represented by the V_s^{30} model.

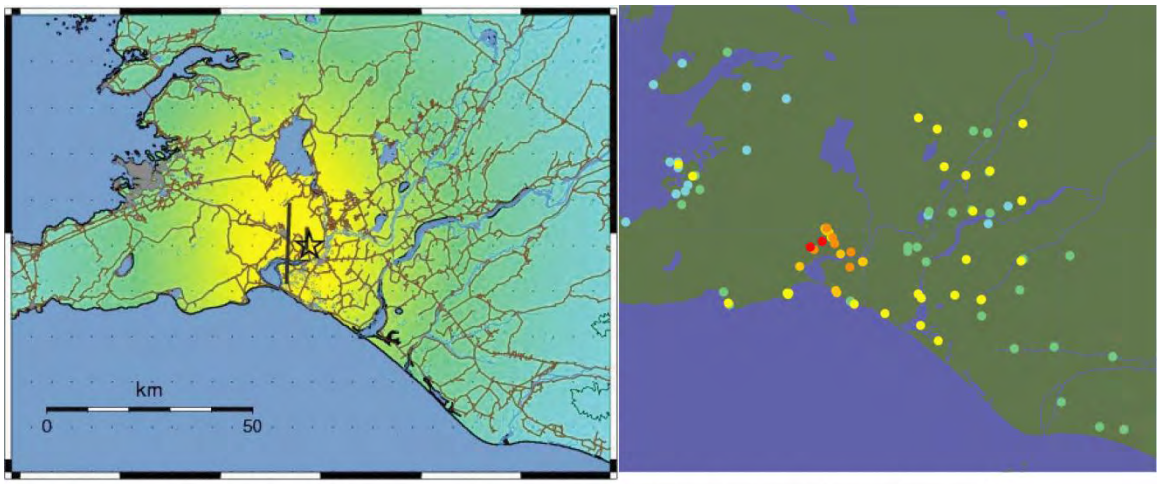

PERCEIVED SHAKING	Not felt	Weak	Light	Moderate	Strong	Very strong	Severe	Violent	Extreme
POTENTIAL DAMAGE	none	none	none	Very light	Light	Moderate	Moderate/Heavy	Heavy	Very Heavy
PEAK ACC.(%g)	*<.17*	*.17-1.4*	*1.4-3.9*	*3.9-9.2*	*9.2-18*	18-34	34-65	65-124	>124
PEAK VEL.(cm/s)	<0.1	0.1-1.1	1.1-3.4	3.4-8.1	*8.1-16*	*16-31*	*31-60*	*60-116*	*>116*
INSTRUMENTAL INTENSITY	I	II-III	IV	V	VI	VII	VIII	IX	X+

Figure 5. (Left) ShakeMap for the M6.3 earthquake in the South Iceland Seismic Zone, near Selfoss on 29 May 2008. The fault ruptured two parallel faults, which have both been incorporated into the ShakeMap. The star marks the rupture initiation on the shorter, eastern fault, which, within seconds triggered rupture on the longer fault, 4 km to the west. (Right) Reported felt intensities in the May 29 earthquake coded with the same colour scheme as the ShakeMap. Comparison shows good agreement between the two maps, except in the epicentral regions, where the ShakeMap underestimates the shaking somewhat.

To implement the USGS ShakeMap software, IMO took advantage of the VMware-Image V1.0.1 installation distributed by project partners at GFZ, Potsdam. The process was installed at month 30 and has been maintained since then, with the information specific to Iceland, such as the attenuation laws and the V_s^{30} map gradually becoming incorporated in the process during the final 6 months of the project. The process will be further adjusted to local site conditions in the coming months and the V_s^{30} velocity model tested, to better approximate the actual observed shaking caused by earthquakes in Iceland. The majority of the sensors in the SIL network are velocity meters, which saturate at around 1.25 cm/s. Therefore in large earthquakes there are sometimes no observations available within 40–60 km epicentral distance. In the future the aim is to install or gain access to more real-time accelerometer data to improve the estimates of near-field ground motions in the ShakeMap for larger earthquakes.

References

Chandler, A. M., Lam, N. T. K. & Tsang, H. H. (2005). Shear wave velocity modelling in crustal rock for seismic hazard analysis. *Soil Dynamics and Earthquake Engineering,* **25**, 167-185, doi:10.1016/j.soildyn.2004.08.005.

Gunnarsson, K., Egilsson, Th., Hafstad, Th., Flóvenz, Ó. G., Stefánsson, S. Ö., Hilmarsson, G. & Thordarson, S. (2005). Berggrunnskönnun á hugsanlegri jarðgangaleið milli lands og Eyja Bylgjubrots- og flugsegulmælingar og athugun á gögnum úr borholum (*e.* Investigation of depth to basement and physical properties of the basement in a region of southern Iceland under consideration for tunnel construction). *Iceland Geosurvey*, *report*, (in Icelandic, with English summary) ÍSOR-2005/033, 45pp.

Pétursson, G. G. & Vogfjörd, K. S. (2009). Attenuation relations for near- and far-field peak ground motion (PGV, PGA) and new magnitude estimates for large earthquakes in SW-Iceland. *Icelandic meteorological Office Report* (in preparation).

Wills, C. J., Petersen, M., Bryant, W. A., Reichle, M., Saucedo, G. J., Tan, S. Taylor, G. & Treiman, J. (2000). A site-conditions map for California based on geology and shear-wave velocity, *Bull. Seism. Soc. Am*., **90**, 6B, S187-S2008.

5. Real-time stress mapping in SW-Iceland

Project no. **036935**

Project acronym: **SAFER**

Project title: **Seismic eArly warning For EuRope**

Instrument: **Specific Targeted Research Project**

Thematic Priority: S**ustainable development, global change and ecosystem priority 6.3.iv.2.1: Reduction of seismic risks**

D5.13 A summary of the performance of EQW algorithm for SW-Iceland

Icelandic Meteorological Office subcontractor:
Ragnar Slunga, Swedish Defence Research Agency, FOI, Stockholm

Assistance with figures by K. S. Vogfjörd

Crustal Stress and Earthquake Prediction Derived from Microearthquake Analysis

A common observation following a large earthquake is that areas experiencing a positive change in Coulomb failure stress (ΔCFS) exhibit increased seismic activity. Still, the predictive value of such an observation is limited by the lack of information of CFS-values before the earthquake causing the change. On the other hand, if the absolute CFS-values are known, the predictive value of the method is greatly increased. In a seismically active region, such as the South Iceland Seismic Zone (SISZ) in Iceland, where the detection threshold of the local seismic network (SIL) is low, tens of thousands of microearthquakes are recorded over the course of a decade. By calculating fault-plane solutions for each event, the distribution of fault-plane solutions in the data set is enough to resolve the stress-tensor- and water-pressure fields. The crustal stress estimates so obtained, can turn the wide-spread ΔCFS-method into a full CFS-method. An algorithm (EQW) to carry out the microearthquake analysis and obtain the stress tensor field at each moment in time will be implemented. This report summarizes the capability of the procedure, when applied to the seismicity recorded in SW-Iceland.

SW-Iceland is the designated area for implementation of the procedures developed within the SAFER project. A map of the region is shown in Figure 1.

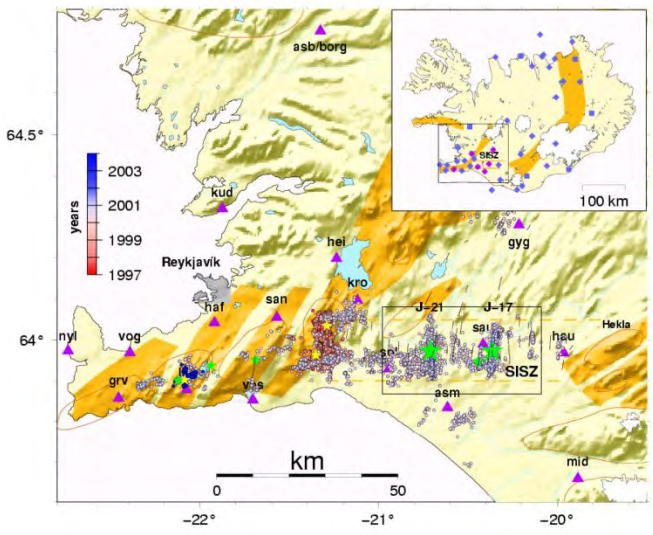

Figure 1. Map of SW-Iceland showing volcanic zones (solid orange) and SISZ (dashed orange). Seismicity on major faults is shown. Stars indicate location of significant earthquakes. The smaller box in the SISZ outlines the region displayed in Figures 2–4.

The box encompassing most of the SISZ represents the analysis area in this study. Analysis of microearthquakes recorded in the SISZ region from the beginning of digital recording, in

1992 up until the origin time of the two M_w6.5 earthquakes in the Seismic Zone on June 17 (J17) and June 21 (J21) 2000 has enabled mapping of the regional stress field in the SISZ prior to the earthquakes. The seismicity during this period is shown in Figure 2. The general results of the microearthquake analysis show that prior to June 17 2000 the shear stress, which is the dominant fault orientation in the SISZ, is highest in the epicentral area of the J17 earthquake; moreover the CFS on N-S oriented, vertical right-lateral strike slip faults is greatest in the epicentral region of the J21 earthquake.

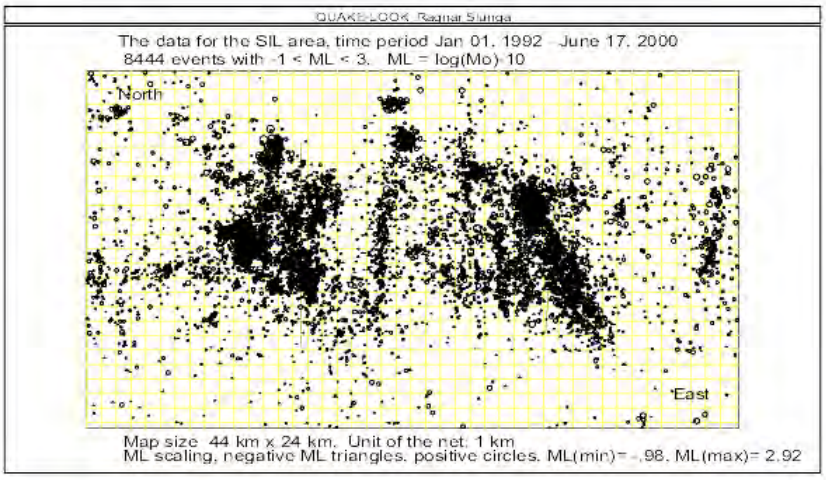

Figure 2. Map of SIL area in SW-Iceland showing recorded seismicity during January 1992 to June 2000.

The results of the microearthquake analysis are summarized in Figures 3 and 4, which show the shear-stress field (Figure 3) and the CFS field (Figure 4) on 44x26 km² maps of the SIL area. Median values of the estimated stress fields at grid points representing 2-km-square boxes, are used to map the stress fields. Each estimate is represented by a circle, scaled by size and is based only on events within the grid-box and independent of its neighbours. The location of the J17 and J21 faults are drawn by red lines. The high shear stress revealed in the J17 epicentral area (Figure 3) shows that the event was an asperity earthquake. After the asperity was breached in the earthquake, the elastic increase in CFS at the epicenter of the J21 earthquake was about 0.3 MPa. This increase may have grown up to 0.6 MPa, after the stress-field change started affecting water flow in cracks. Figure 3 shows that prior to the J17 event, the CFS field in the J21 epicenral area is -0.7MPa. An instantaneous increase of 0.3MPa due to the first earthquake, followed by a further increase due to the water flow, would bring the CFS field close to zero and thus trigger failure. The 3-day delay of the J21 earthquake is therefore most likely explained by the water flow effects.

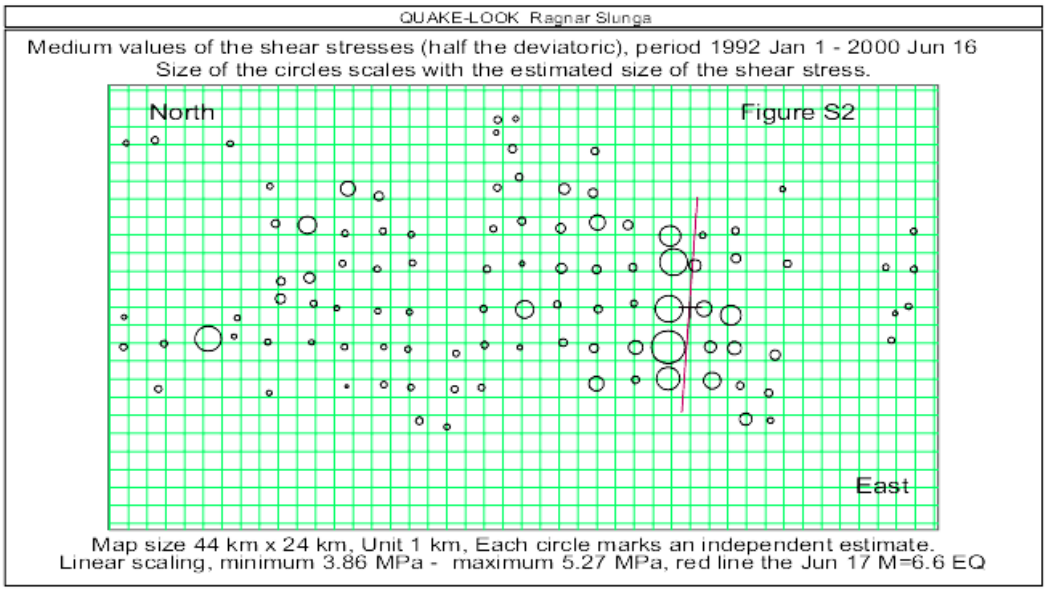

Figure 3. Median values of shear stress in the SIL region, for the period Jan. 1992 – June 16 2000. The largest deviatoric stresses fall along, and within 1–2 km of the J17 fault trace, which is marked with a red line. The figure clearly shows that the J17 event was an asperity earthquake, and that its position could have been predicted on the basis of the stress analysis.

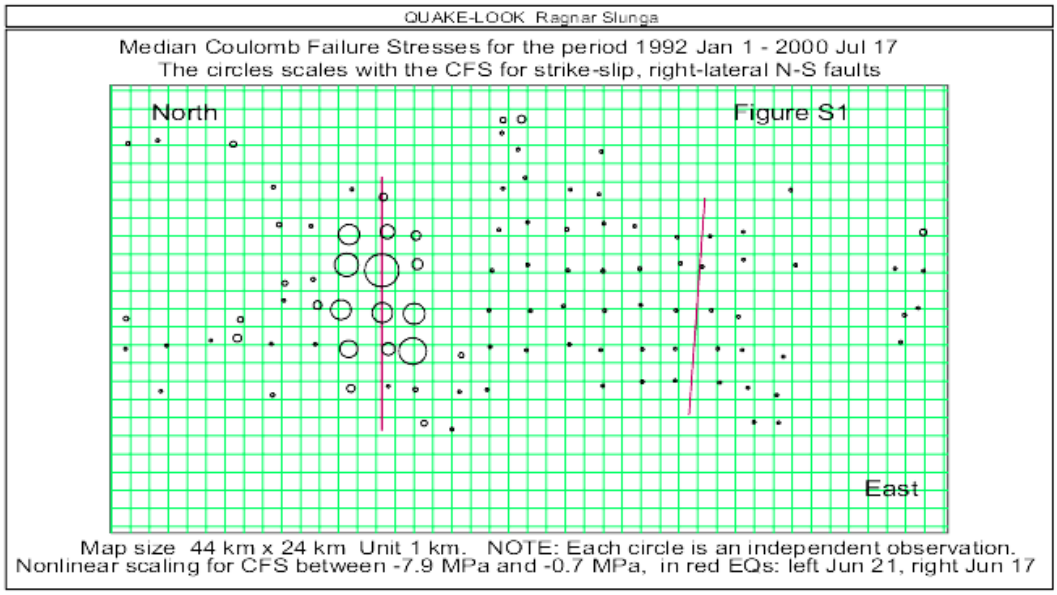

Figure 4 Median values of the CFS field in the SIL area prior to the J17 earthquake. Values range from -7.9MPa to -0.7MPa, with the -0.7MPa values aligning along the fault trace of the J21 event shown by the red line on the left. With the increase in CFS caused by the J17 event, these values are brought closer to zero and thus failure.

The results presented show that good estimates of the absolute crustal stress tensor can be achieved by analysis of microearthquakes and that by utilizing information about the stress field carried by previously recorded microseismicity, the location of the June 17 2000 earthquake in the SISZ could have been predicted. Furthermore, after the earthquake struck, as soon as its magnitude and mechanism became known (or could be guessed!), an increase in CFS of about 0.6 MPa could have been anticipated to occur within a few days at the J21 epicenter. Knowing that the median CFS at the J21 epicenter was already -0.7 MPa it is obvious that the probability for the J21 earthquake to occur within a few days was quite high, and a warning could have been issued. Use of absolute crustal stress in this manner should improve advance earthquake warnings.

Further work is concentrated on making automatic updating of the stress tensor field and especially the CFS field for known earthquake zones. The stress fields will be easily accessible by the other monitoring software at IMO. The first steps to such an automatic software has been taken and tested. The work is progressing according to the planned time scale.

Project no. **036935**

Project acronym: **SAFER**

Project title: **Seismic eArly warning For EuRope**

Instrument : **Specific Targeted Research Project**

Thematic Priority: S**ustainable development, global change and ecosystem priority 6.3.iv.2.1: Reduction of seismic risks**

D5.14 Implementation of EQW at the Icelandic test site

Icelandic Meteorological Office subcontractor:
Ragnar Slunga, QuakeLook Stockholm, Stockholm, Sweden (ragnar.slunga@telia.com)

Assistance and editing of figures by G. B. Gudmundsson and K. S. Vogfjörd

Implementation of EQW at the Icelandic test site

Introduction

Crustal stresses can be expected to be of major importance for any prediction of crustal deformations. A method for monitoring the crustal stresses, based on analysis of microearthquakes is applied to southwest Iceland, which is defined as the SAFER testing region. The region includes the South Iceland Seismic Zone (SISZ), where a series of significant earthquakes (M>6) have occurred over the last millennium, and the Reykjanes peninsula, which also has experienced repeated significant earthquakes, as well as volcanic eruptions. The SISZ is currently undergoing a major earthquake sequence, which started in June 2000 with two, M6.4 and M6.5 earthquakes followed by a M6.4 earthquake in May 2008. The first earthquake in June 2000, dynamically triggered two additional and significant earthquakes (M>5.5) at 70 km distance on Reykjanes peninsula. More large earthquakes are expected in the zone in the coming years.

Estimation of the stress tensor causing a microearthquake

For a homogeneous isotropic rock mass having a shear slip failure, the Coulomb criterion puts four constraints on the stress tensor causing the shear failure. For a rock mass having one fracture McKenzie (1969) came to the conclusion that only very weak constraints could be put on the stress tensor from the observation of the shear slip. One implicit assumption behind the conclusion of McKenzie was that the stress tensor field was not limited by fractures in the rock mass. As this implicit assumption was not clearly presented it has been rather generally accepted that the conclusion was correct. However, already in 1978 it was becoming clear that the rock stresses are constrained by the frequent fractures in the crust (Jamison and Cook, 1978) and later, this was clearly confirmed by Slunga (1988). It seems that this important observation was not everywhere noticed. Instead a nice way to formally put four constraints on the rock stress tensor by use of Bott's criterion was presented by Angelier (1979) and by Gephart and Forsythe (1984). The physical drawback with the methods based on Bott's criterion was that they required that slip on four differently oriented fractures were due to the same stress tensor. This is of course wrong from a physical point of view (assumes that slip occurs with non-zero Coulomb Failure Stress (CFS)). In addition it seems highly unlikely that the stress is homogeneous enough in a fractured volume undergoing frequent shear slips.

The method developed herein avoids the physical problems by using the Coulomb failure model as a good approximation for the failure in the fractured crust, as the rock mass contains numerous fractures at all scales. This means that one single microearthquake can be used to put four constraints on the rock's stress tensor. This method, which achieves in situ stresses from microearthquakes, has great commercial value within mining, geothermal energy and for operations in oil- and gas fields. For this reason all details of the method will not be given here, but briefly the steps are the following: First the use of Coulomb failure criterion for the fractured crust requires that the water pressure be known. For the shallow crust, having fluid connection to the surface the water pressure will be hydrostatic and for the deeper crust, the limited strength of the rock will give water pressure related to the lithostatic pressure. Secondly rock stress measurements have shown that the vertical stress equals the lithostatic

pressure, with small differences. The use of Coulomb failure criterion instead of Bott's criterion means that we are working with the singular case for the Bott's criterion, see Gephart (1985). By handling this singularity in a careful way the remaining degree of freedom is eliminated and the whole stress tensor is determined from the analysis of a single microearthquake. It is worth noting that the method implicitly discriminates the fault plane and the auxiliary plane, which is causing some troubles in the methods using Bott's criterion.

Due to the commercial value of the method, it is patent pended globally. However, for earthquake warning QuakeLook Stockholm AB is offering a non-commercial cooperation with implementation of the earthquake warning. The implementation at IMO, Reykjavik is based on such cooperation. Interested partners can contact Ragnar Slunga at QuakeLook Stockholm AB by phone +46 (0)703773507 or by email ragnar.slunga@telia.com.

Apparent stresses and the QuakeLook EQW algorithm implemented at IMO

The fault volume of a large earthquake is roughly $2 \times 5 \times 10$ km^3 giving 100 km^3. The volume of a microearthquake is less than 0.001 km^3. Thus there are 100,000 places for microearthquakes within the fault volume. It is obvious that a few random observations of the stress within the fault volume may give very scattered result. However, the microearthquakes occurring during a given time period are certainly not randomly picked, especially not during periods of increased activity. In fact the fault plane solutions (FPS) of the microearthquakes within a given time period are likely to reflect the change of the crustal stability during the period. If the CFS for large earthquakes is increasing there will be a tendency for the triggered microearthquakes to have FPS's consistent with this. Thus it is expected to observe before the earthquake, a rapidly increasing apparent CFS consistent with the mechanism of the major earthquake. The dependency of the stress estimates on the crustal loading during the time of observation motivates the use of the term apparent, especially when the median value is estimated from few events or short time windows.

Use of few microearthquakes for the estimate of the apparent CFS (corresponding to a typical mechanism of the large earthquakes) can give a large scatter. On the other hand the foreshocks are sometimes quite few so a compromise is needed. The simplest way to make a good choice is to study the behaviour when using different numbers of events. The exact way of how to use the apparent stresses for short term earthquake warnings must be tested with the actual microearthquake data.

The QuakeLook algorithm allows for a free choice of the number of microearthquakes required for a stress estimate to be performed. The output contains the size of the shear stress (half the deviatoric stress) and the CFS for N-S, strike-slip, right-lateral vertical faults, which is the dominant mechanism of major earthquakes in the South Iceland Seismic Zone. The shear stress is included, because it indicates places of large elastic energy, and the size of the high stress volume can possibly indicate the possible size of a coming EARTHQUAKE. In addition to the number of microearthquakes used for the estimates, one also has to specify three instances of time: the start and end times of the time interval analyzed (T2=duration of time interval), and the number of days (T1) before the end time, for which large observed stresses are assumed to be of value for earthquake warnings.

For earthquake warnings we also needed to know whether the apparent CFS is increasing or not, and if increasing, when the earthquake will come. For that purpose the observed CFS values at the position of all microearthquakes recorded during the later time window (T1) are compared with the corresponding CFS values for the earlier part of the total time window (T2). From this difference a linear trend is assumed and the time when zero CFS is reached, is the formal extrapolated time of the coming earthquake, at that site. This is not an effort to predict earthquakes, it is just a way to make the analyst aware of the possible danger.

Some results of tests with the QuakeLook EQW algorithm

The output of the QuakeLook EQWA algorithm implemented at the Icelandic meteorological Office (IMO) consists of one text-file and three graphic files (maps) showing the apparent shear stresses, the apparent CFS for the SAFER region of Iceland, which includes the South Iceland Seismic Zone (SISZ), and the places which are most likely to have the next earthquake, based on the number of days to reach CFS instability. This computation is just a simple linear extrapolation and is not a real forecast, but a rough, formal way to indicate the present rate of increase in a simply understood way.

The method is quite new and little experience is so far available. The early tests show surprisingly stable behaviour, even when the estimates are based on quite few events. Actually, even only one event seems often to be of value, even if such estimates in themselves are scattered. Together with estimates based on more events and/or other methods and information the value of the method is of course increased.

Before the June 17 2000 Mw=6.4 earthquake

On June 11 2000, a place at longitude -20.35E started to show increasing CFS. The situation remained rather constant until the earthquake at 15:41 GMT on June 17. The apparent shear stress, apparent CFS, and extrapolated time to instability evaluated at 12:00 GMT on June 17, roughly three hours before the earthquake is shown in Figure 1. The values are obtained using four events (N) recorded during the preceding 21 days (T1) and compared to median values from the preceding 18 months (T2). The grey scale for shear stress spans 5.8 to 12.3 MPa. Note the high stresses at the epicenter, this has been observed for years (since the beginning of the SIL network in 1992). One interesting feature in the CFS mapping is the large values observed south of the fault. The grey scale for CFS spans -12.8 to -1.25 MPa. Note the consistent CFS increases at the fault before the earthquakes. Using the median of 4 events (N=4), the time to instability is about 3 months. If N=1 is used (Figure 2) the estimated time to instability becomes 33 days and increasing CFS is also observed on the June 21 fault.

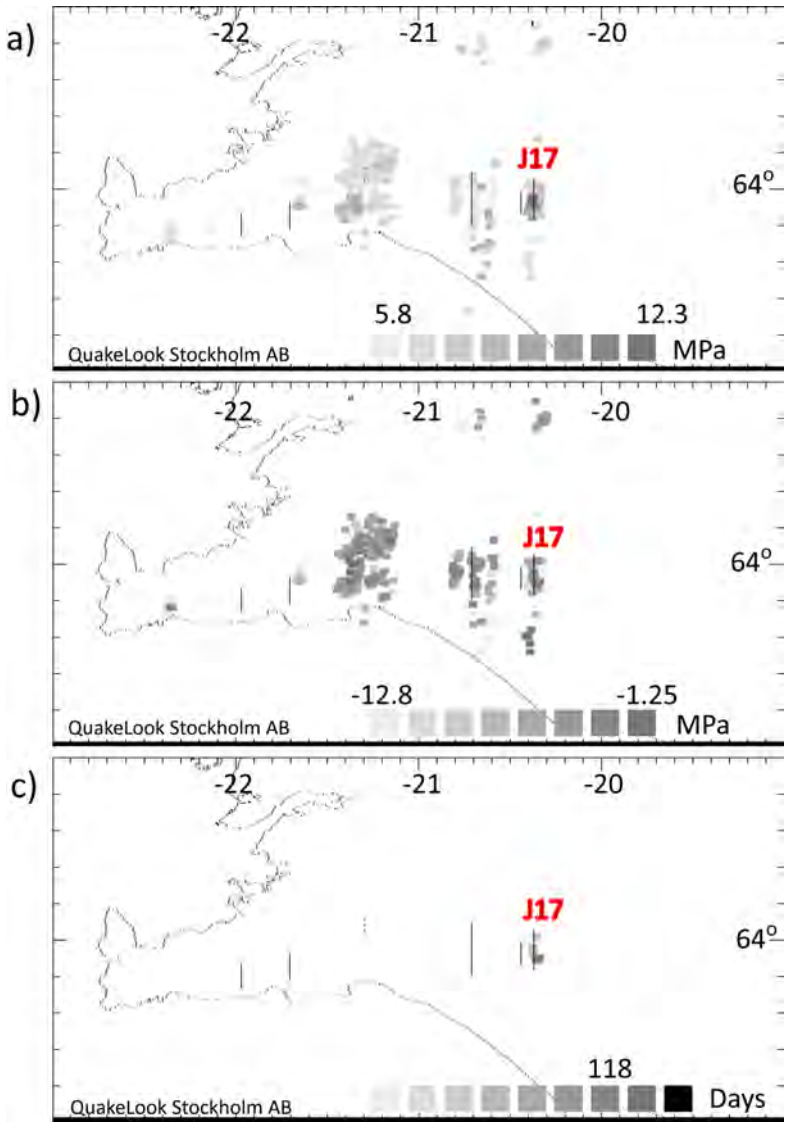

Figure 1. Maps of southwest Iceland showing stress estimations made at 12:00 GMT on June 17 2000, roughly 3 hours before the June 17 earthquake. The figure shows: (a) apparent shear stress (b) apparent Coulomb failure stress (CFS) and (c) extrapolated time to instability. The parameters used in the estimate are: N=4, T1=21 days, T2=18 months. Stress values are only estimated at locations with the minimum number of events (N=4) over the preceding 21 days (T1). Darker squares in a, and b, indicate higher stress values; in c darker means shorter time. Faults of major events activated on June 17 and 21 are shown by black N-S oriented lines.

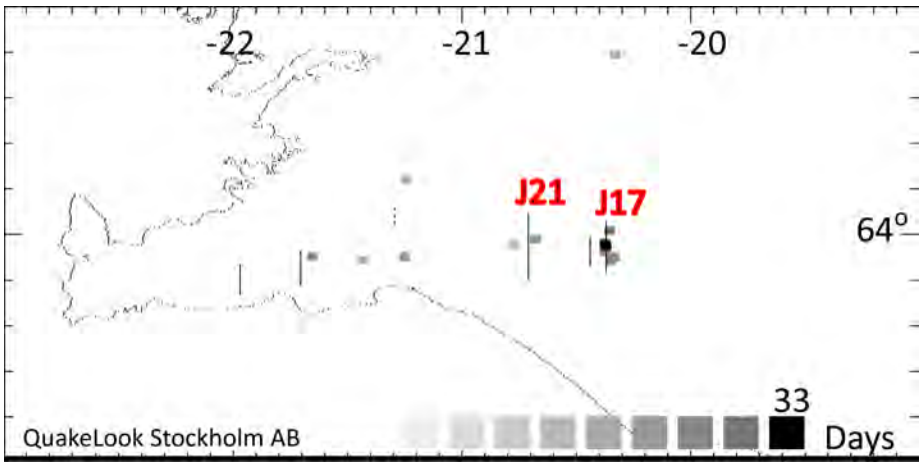

Figure 2. Same as Figure 1c, except with N=1.

Before the June 21 2000 Mw=6.5 earthquake

The June 21 earthquake occurred only 3.5 days after the June 17 earthquake. This motivates the use of short time intervals, because everything was changed by the June 17 event. Figure 3 shows the places of increasing CFS. The clustered indications at the fault of the June 21 event (solid line) indicate failure in 1.3 days. The map was computed based on data up to 21:00 GMT on June 20. The earthquake occurred 4 hours later.

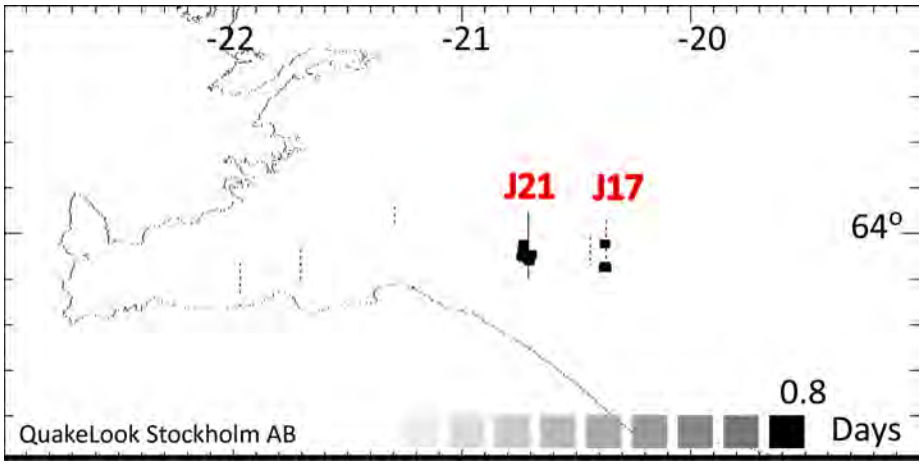

Figure 3. Map of southwest Iceland showing places with increasing Coulomb failure stress (CFS) evaluated at 21:00 GMT on June 20 2000, roughly 4 hours before the June 21 earthquake. The parameters used in the estimate are: N=4 events, T1=1 day, T2=3 days. Faults activated on June 17 are shown by black dashed N-S oriented lines, while the June 21 fault is shown with a solid line. Darker squares indicate shorter time to instability.

Table 1 shows the text output which one gets from the stress analysis tool in addition to the figure files. This is the output described above. Note that the "false" alarms (largest apparent CFS) is on the previous fault. This is quite common. Note also that the shortest time to failure is at a place where the apparent CFS is less than -3 MPa which reduces its present importance. The June 17 earthquake triggered activity in many different places giving such effects.

Table 1. Stress estimates made at 21:00 on June 20 2000, 4 hours before the June 21 earthquake taking the median values of the last 4 events recorded during the last day and comparing them to the median values obtained during the preceding 3 days.

N=4 T1=1 day
Time interval 000617 1800 000620 2100

Produced by QuakeLook Stockholm AB
Ragnar Slunga +46 (0)703773507

Apparent Coulomb Failure Stress, MPa: min -17.6 MPa max -.72 MPa

	CFS	latitude	longitude	time to zero	
	MPa	N	E	days	comment
Places	-.721	63.929	-20.367	1.0	000617 fault
Places	-.721	63.977	-20.367	1.0	000617 fault
Places	-1.207	63.947	-20.724	1.2	
Places	-1.207	63.976	-20.721	2.6	
Places	-1.293	64.063	-21.160	99999.0	

Days to zero (rough figures): 1000000.0 .8 days -3.046 MPa
At position 63.977 -20.438

Apparent shear stress range, MPa: min 5.92 MPa max 11.63 MPa

	Shear stress	latitude	longitude
	MPa	N	E
Places	11.631	63.958	-20.345
Places	11.631	63.979	-20.344
Places	11.631	63.941	-20.345
Places	11.284	63.957	-20.150
Places	11.284	64.292	-20.308
Places	11.284	64.391	-20.296
Places	11.284	64.274	-20.306
Places	11.284	64.306	-20.296
Places	11.246	64.017	-20.360
Places	11.246	64.038	-20.361
Places	10.821	64.016	-20.413
Places	10.821	63.982	-20.423

Before the May 29 2008 Mw=6.3 earthquake

The May 29 earthquake occurred on two faults (solid in Figure 4) and started on the shorter eastern fault. It was preceded by foreshocks during the preceding night, but an increase in CFS was not observed at the epicenter until at 11:50 GMT on May 29. With N=1 the failure was expected after 8 days. Later in the afternoon, at 15:00 GMT, similar analysis gave the estimated time to failure to be 1.3 days. The apparent CFS at 15:00 GMT on May 29 is shown in Figure 4 and one can see that the largest apparent CFS is found at the right fault (CFS = -0.42 MPa) and rather high values are also indicated at the second, longer fault. The places of increasing CFS all around the starting fault are shown in Figure 4b.

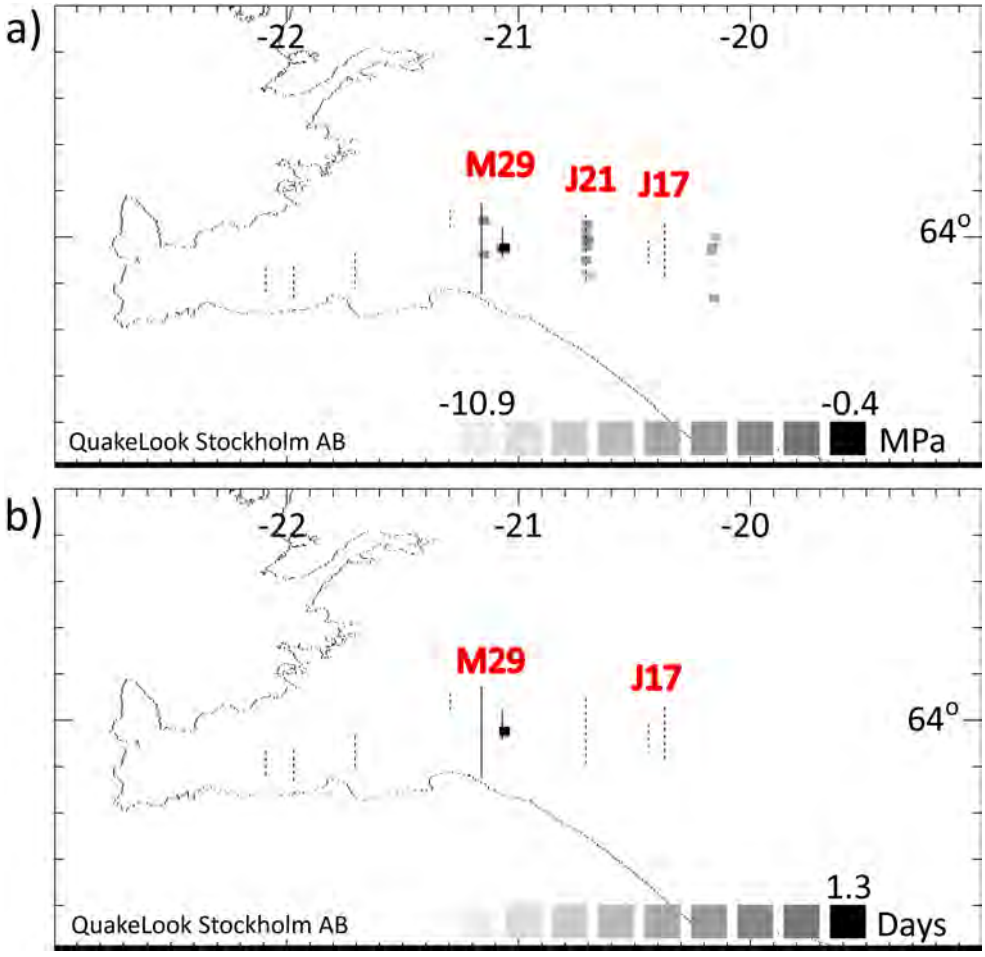

Figure 4. Maps of southwest Iceland showing stress estimations, made at 15:00 GMT on May 29 2008, 45 minutes before the May 29 earthquake. The figure shows: (a) apparent Coulomb failure stress (CFS) and (b) extrapolated time to instability. The parameters used in the estimate are: N=1 event, T1=1 day, T2=1 year. Stress values are only estimated at locations with one event during the preceding one day. Darker squares in a, indicate higher stress values; in b, darker means shorter time to failure. Faults of major events activated in 2000 are shown by dashed black N-S oriented lines. The fault traces of the two coming faults are shown with black solid lines.

Discussion

There are three free parameters in the EQWA method. It is well known that any method with any free parameter can easily be overvalued. The free parameters are the number of microearthquakes (N) needed for an estimate, the length of the time period before the present (T1) used to obtain the present value, and the length of the preceding time period (T2), before T1, which is used to estimate the previous value.

If there is a random component in the observations of the microearthquake fault plane solutions (FPS), then it is obvious that if T2 is large enough the previous value may be so large that any increase in CFS can hardly be detected. Thus T2 should not be too large. A large T2 increases the probability that a dangerous rise in CFS is missed (especially with small N), whereas a small T2 increases the number of random alarms. On the other hand, if T1 is large, the predictive value of the observation is lost, thus T1 should in some way be chosen properly.

Experience from testing on SISZ earthquakes has shown that even N=1 gives rather stable results and may be valuable for short term warnings. Normally such a small N should not be used, unless larger N-values, say 4-12, support the N=1 observation.

For estimates of the crustal stress one should use a long T1 window and a large number N. In addition, the activity within the period should not be too clustered in time. The reason is that any short time window may be influenced by very special tectonic loading at the place of interest and may therefore give a biased median value.

The basic view behind this way of using the stress monitoring tool for warnings is as follows: The argument that any small microearthquake can start a large earthquake is most likely not true. Only a few can be the beginning of something big. That is why we have 300,000 microearthquakes and only a handful of large earthquakes detected in Iceland since 1990. However, the foreshocks which occur at the place of an oncoming earthquake, and which have mechanisms similar to that of the main event can a priori all be seen as the start of the main event. So far, only one earthquake of about ten events along the SISZ has come without any detected foreshock. This means that the number of foreshocks is typically in the range 5-40. Therefore, the number N should be chosen to be so small, that N foreshocks will occur before the one starting the large event occurs. If this attempt is successful, it will be possible to anticipate the main event and this motivates the use of small N, and even single events. During the continued routine use of the tool, experience will show the amount of false indications as a function of N.

Note that implicit in the method is that the increased activity before an earthquake may lead to "correct" but random warnings. The results are, however, much better than expected due to this random effect. The increased activity mainly assures that there will be appropriate observations.

The evaluation procedure is being installed in such a manner that it can be used in day-to-day operations by IMO’s personnel responsible for monitoring seismic activity in Iceland.

Acknowledgements

Thanks to Gunnar B. Gudmundsson and Kristín S. Vogfjörd for making the maps and various contbution.

References

Angelier, J. (1979). Determination of the mean principal directions of stresses for a given fault population. Tectonophysics, 56, T17-T26.

Bott, M.H.P. (1959). The mechanics of oblique slip. *Geological Magazine*, 96, no 2, 109-117.

Gephart, J.W. (1985). Principal stress directions and the ambiguity in fault plane identification from focal mechanisms. Bull. Seism. Soc. Am., 75, pp 621-625.

Gephart, J. & Forsyth, D. (1984). An improved method for determining the regional stress tensor using earthquake focal mechanism data: application to the San Fernando earthquake sequence. *J. Geophys. Res*. 89, pp. 9305–9320.

Jamison, D.B. & Cook, N. G. W. (1978). An analysis of the measured values for the state of stress in the earth's crust. Techn. proj. rep. no 7, LBL-7071, SAC-07, Lawrence Berkeley Laboratory and University of California, Berkeley.

Jamison, D. B. & Cook, N. G. W. (1980). Note on measured values for the state of stress in the earth's crust, *J. Geophys. Res*., 85(B4), 1833-1838..

McKenzie, D.P. (1969). The relation between fault plane solutions for earthquakes and the directions of principal stresses. *Bull. Seism. Soc. Am*., 59, 591-601.

Slunga, R. (1988). Frictional Sliding and the Crustal Stresses. In: *Deep Drilling in Crystalline Bedrock*, Vol. 2, Proceedings of the International Symposium held in Mora and Orsa, Sept 7-10, 1987. Editors Boden A. and K.G. Eriksson, Springer-Verlag, Berlin.